JOC The Journal of Organic Chemistry

Article

pubs.acs.org/joc

p,p-Dihydroxydihydrostilbenophanes Related to Antimitotic Combretastatins. Conformational Analysis and Its Relationship to Tubulin Inhibition

Raquel Álvarez,[†,‡] Vilmarí López,[†] Carmen Mateo,[†] Manuel Medarde,[†,‡] and Rafael Peláez*[,†,‡]

[†]Laboratorio de Química Orgánica y Farmacéutica, Facultad de Farmacia, Universidad de Salamanca, Campus Miguel de Unamuno, E-37007 Salamanca, Spain

[‡]Instituto de Investigación Biomédica de Salamanca (IBSAL) and Centro de Investigación de Enfermedades Tropicales de la Universidad de Salamanca (CIETUS), E-37007 Salamanca, Spain

Supporting Information

ABSTRACT: The structures of a new family of macrocyclic analogues of combretastatins B combining oxygenated substituents on the phenyl rings and indole rings are described. The effects of the stereochemistry, of the length of the spacer linking both aryl groups, and of the decoration of the macrocycles on the kinematics of the system have been studied by means of NMR studies at several temperatures and in different solvents combined with theoretical studies including Monte Carlo conformational searches and molecular dynamics simulations at different temperatures. The new indole macrocycles provide a more rigid view of this kind of macrocycles than that previously held. The tubulin polymerization activity of this new class of macrocycles has been assayed and analyzed.

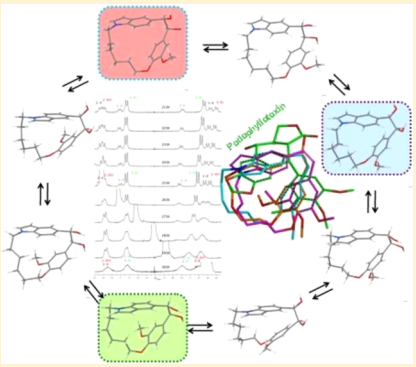

INTRODUCTION

Combretastatins are cytotoxic natural products originally isolated from *Combretum caffrum*.[1] Combretastatins A–C are biosynthetically related stilbenes, dihydrostilbenes, and phenanthrenes and dihydrophenanthrenes,[2] respectively, while combretastatins D are unrelated 15-membered diaryl ether macrolactones.[3] Combretastatin itself is a 1,2-diphenylethanol.[4] Combretastatins A, e.g., combretastatin A-4 (CA-4), and related analogues have attracted great attention due to their advance into clinical trials as antitumor compounds.[5] Combretastatins bind at the colchicine site of tubulin, alter tubulin polymerization dynamics, and inhibit microtubule formation.[2a] Tubulin inhibition often results in cytotoxic activity and disruption of tumor specific vasculature, but combretastatins have stood out from most of other inhibitors because they destroy tumor neovasculature well below their maximum tolerated doses.[6] The origin of this advantage is presently unknown, but differences in binding to tubulin, in pharmacokinetics, or the existence of additional, presently unknown targets have been suggested.[7] Combretastatins suffer from two major drawbacks: low water solubility and chemical instability arising from the ready isomerization to the thermodynamically more stable but inactive *trans* isomers. The main strategies applied to overcome the low water solubility have been the introduction of solubility-increasing polar groups and the preparation of prodrugs.[7] The chemical instability has been addressed by introducing modifications on the bridge between the two phenyl rings and by the formation of macrocycles (Figure 1).[7−9]

Combretastatins B are less potent than combretastatins A.[10] This is often attributed to the penalty associated with the adoption of a cisoid disposition in the bound conformation.[11] Nevertheless, several modifications on the ethane bridge, such as hydroxy groups or its inclusion in small rings, lead to potent inhibitors of tubulin polymerization.[12] The bridge-modified analogues are particularly interesting as they reduce the highly lipophilic character of the stilbenes, thus increasing their aqueous solubility, and also provide anchor points for further derivatization. This second possibility is particularly interesting, as these substituents likely bind to tubulin close to where the hydroxy group of podophyllotoxin or the amide group of colchicine do, pointing toward a solvent exposed cavity.[13] Therefore, the achievement of conformationally restricted combretastatin B analogues is a highly desired goal.

Macrocycles are rings of 12 or more atoms. More than 100 macrocyclic natural products have reached the market, but the application of macrocycles in drug discovery has been limited due to anticipated synthetic difficulties and concerns about their druglike properties.[14] Macrocyclic molecules, although conformationally restricted, are by no means rigid. In favorable cases, this reduces their accessible conformational space while allowing a certain degree of fit when interacting with their

Received: April 8, 2014
Published: June 26, 2014

 © 2014 American Chemical Society

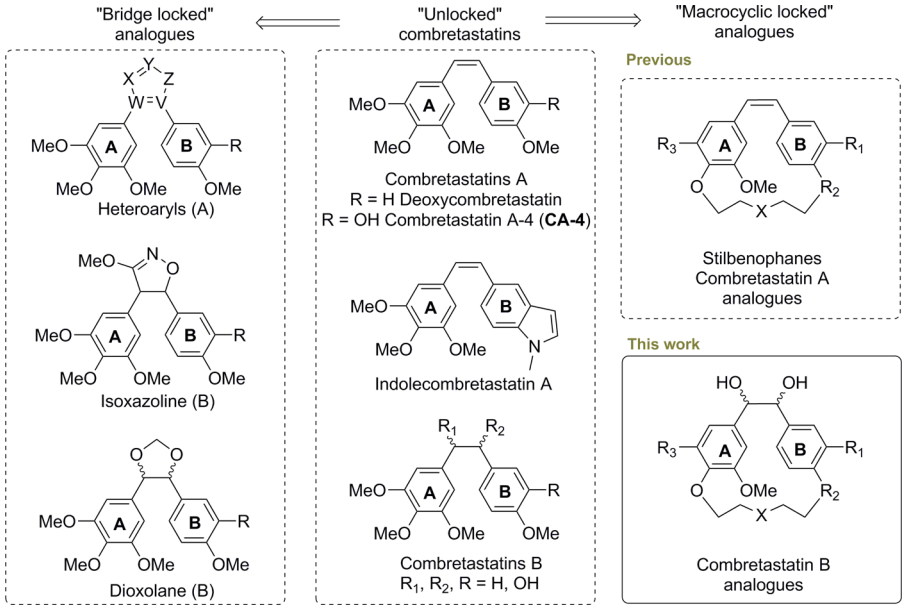

Figure 1. Strategies employed to lock combretastatins in a *cisoid* disposition by preventing *Z* to *E* isomerization of combretastatins A or by conformational restriction of combretastatins B. In both cases, this can be accomplished by modifying the bridge (left panel) or by the formation of macrocycles (right panel). Right panels: R_1 = H/OMe, R_2 = O, R_3 = H/OMe, X = O/CH_2CH_2 or R_1–R_2 = −CH═CH−N−, R_3 = H/OMe, X = CH_2CH_2.

Scheme 1. Synthetic Methodology (for Details, See Previous Papers)

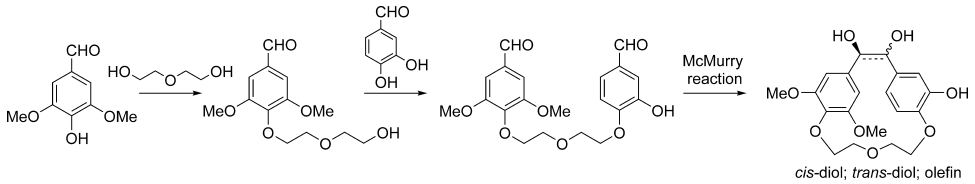

targets. Therefore, macrocycles can be used to improve the pharmacodynamics, such as potency and selectivity, or pharmacokinetics, such as stability or permeability, of drug candidates. We have recently applied this methodology to combretastatins A with the aim of preventing the undesired *cis*–*trans* isomerization, and we have designed, synthesized, and evaluated a family of polymethoxylated stilbenophanes along with new analogues carrying an indole B ring.[9] Although less potent than their open-chain analogues, these compounds were the first macrocyclic combretastatin A analogues that inhibited tubulin polymerization and served as a proof of concept. For these macrocyclic combretastatin A analogues, the accessible conformational space played a very important role in the biological responses obtained. The final McMurry coupling employed as the last step of the synthetic route to the macrocyclic combretastatins produced not only the macrocyclic analogues of combretastatins A but also the corresponding dihydro–dihydroxy combretastatin analogues. These dihydro derivatives are characterized by the observation of conformational equilibria at room temperature or at low temperature and by the appearance of multiple observable conformations in the more rigid structures, which could not be observed in the more flexible ones due to fast conformational exchange. In this paper, we describe and discuss the conformational preferences of macrocyclic combretastatin B analogues, already obtained by us,[9] and how they could affect their biological effect.

RESULTS AND DISCUSSION

Synthesis. The macrocyclic diols were obtained together with the stilbenophanes, as has been previously described.[9] In brief, two consecutive alkylations of adequate phenolic (indolic) aldehydes with the required reactive linker moiety produced intermediate dialdehydes, which were subjected to McMurry internal coupling at room temperature or under reflux.[9] This sequence, comprising a regioselective Mitsunobu alkylation of the *p*-hydroxy group of catechol,[15] is shown in Scheme 1 for compounds **1** and **2** and their olefin.

The results of the McMurry olefinations and pinacol couplings vary depending on the structure of the dialdehydic precursor and the reaction conditions.[9] Obtained diols **1**–**10** and their acetylated derivatives are shown in Figure 2.

Stereochemical Assignment. The diols or diacetates **1**–**10a** have been assigned the "*cis*" or the "*trans*" configurations based on key differences in their ^{1}H and ^{13}C NMR data following the trends previously observed for related systems with two axially symmetric phenyl rings[9] and literature on 1,2-diols.[16] (All the assignments have been based on 2D-NMR spectra (HSQC, HMBC, COSY, NOESY, and/or ROESY) and compared with those of related macrocycles previously obtained by us). The chemical shifts of the bridge protons and carbons and the coupling constants between the bridge protons serve to assign the relative configuration, as summarized in Table 1.

Although the application of these rules to compounds lacking the symmetry of both rings is much more difficult, the empirical

dx.doi.org/10.1021/jo500798r | J. Org. Chem. 2014, 79, 6840–6857

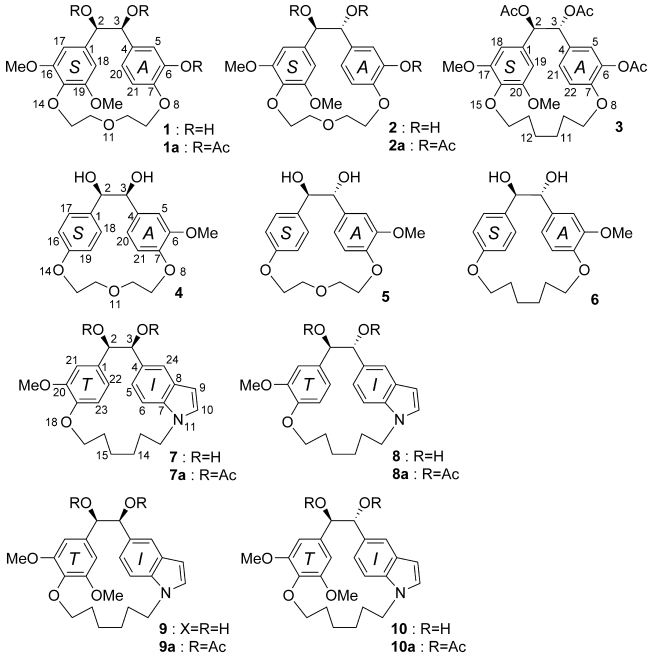

Figure 2. Structures of diols and acetyl derivatives. Rings have been labeled in compounds **1**−**6** as S, symmetric, and A, asymmetric, and in compounds **7**−**10a** as I, indolic, and T, tri- or tetrasubstituted (trisubstituted for compounds **7**−**8a** and tetrasubstituted for compounds **9**−**10a**). All of them have one symmetric and one asymmetric ring except **7**−**8a**, which are double-asymmetric.

Table 1. Empirical Rules Deduced for Stereochemical Assignment of "*Erythro*"-"*Cis*" or "*Threo*"-"*Trans*" Configurations for this Class of Diols[a]

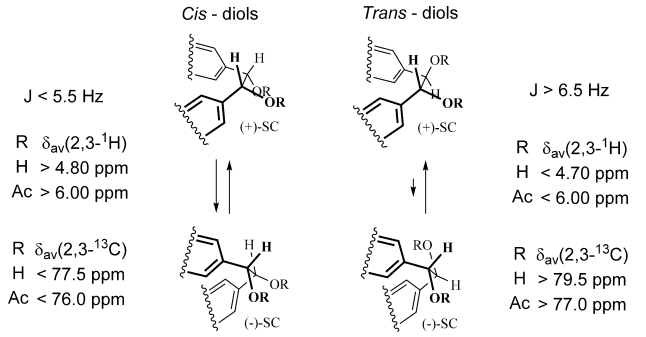

[a](+)SC and (−)SC stand for positive and negative bridge synclinals.

rules for the assignment of the relative stereochemistry of the diols presented in Table 1 are fulfilled by compounds **1**−**10a**. When different conformations are observed under the cited conditions for a given compound they also adhere to the rules, as can be appreciated for **1** and **2** in Table 2 (for ^{1}H NMR); larger chemical shifts and smaller coupling constants are always observed for H-2 and H-3 of the *cis* isomers in comparison with the *trans* isomers. Furthermore, the ^{13}C chemical shifts of the bridge methines (C-2 and C-3) are always higher for the *trans* isomers than for the *cis* isomers. A complete comparison for compounds **1**−**10** is included in the Supporting Information.

Conformational Analysis of Diols. For previously described symmetrically substituted phenyl rings, diols, or acetates,[9] ring rotations result in chemically identical structures. This reduces the number of observable conformations for these macrocycles to the synclinal dispositions of the bridge as

Table 2. ^{1}H NMR and ^{13}C NMR Data for CH-2 and CH-3 of Compounds 1 and 2 with Two Observable Conformations in $CDCl_3$ at rt

cis	%[a]	H-2	H-3	avg[b]	(*d*)[c]	C-2	C-3	avg
1	55	4.79	4.87	**4.83**	(5.1)	75.6	75.7	**75.6**
1	45	4.79	4.88	**4.83**	(5.1)	76.0	75.2	**75.6**
trans	%[a]	H-2	H-3	avg[b]	(*d*)[c]	C-2	C-3	avg
2	70	4.46	4.51	**4.49**	(7.4)	82.3	81.6	**81.9**
2	30	4.52	4.58	**4.54**	(6.7)	82.4	81.6	**82.0**

[a]%: percentage of each observed conformer. [b]avg: average shift of H-2 and H-3 for each compound/conformation. [c](*d*): coupling constant observed for doublets of H-2 and H-3.

evidence NMR spectra with a single set of signals. Now we have introduced in the system one or two asymmetrically substituted aromatics, which results in an increase in the number of chemically different observable conformations. As a result, the conformational equilibria in this series and their NMR spectra are more complex.

For a detailed conformational analysis we have considered the possibilities depicted in Figure 3 for the conformational

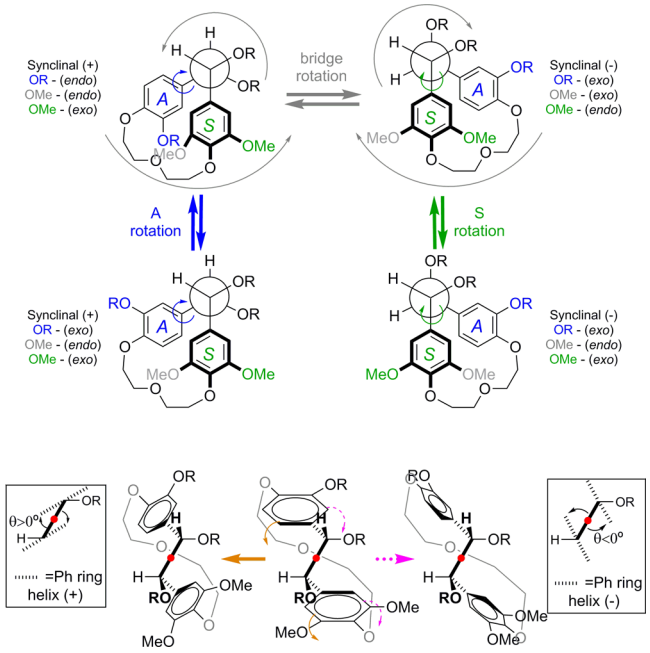

Figure 3. Motions implicated in the genesis of conformational possibilities of diols (represented by triol **1** and triacetate **1a**): A-ring (left) and S-ring (right) rotations, bridge rotation (+ and − synclinal exchange, horizontal), can take place. Incomplete ring rotations are denoted as helicity (axis indicated by a red dot) changes (bottom equilibria).

exchange: bridge rotations (in the horizontal) between two synclinal conformations, rotation of one or the other aromatic rings (in vertical), and changes in the helicity (bottom equilibrium). The helicity changes (Figure 3, bottom) can be thought of as changes in the helical sign of the individual blades of a propeller and are associated with changes in the sign of the dihedral angle between the plane of each aromatic ring and the central bond (Csp^3−Csp^3) of the bridge, without passing any ring plane through the intra-annular space. The helical signs of both aromatic rings usually match, and then the conformations are assigned that sign (Figure 3, bottom framed images). The

dx.doi.org/10.1021/jo500798r | J. Org. Chem. 2014, 79, 6840−6857

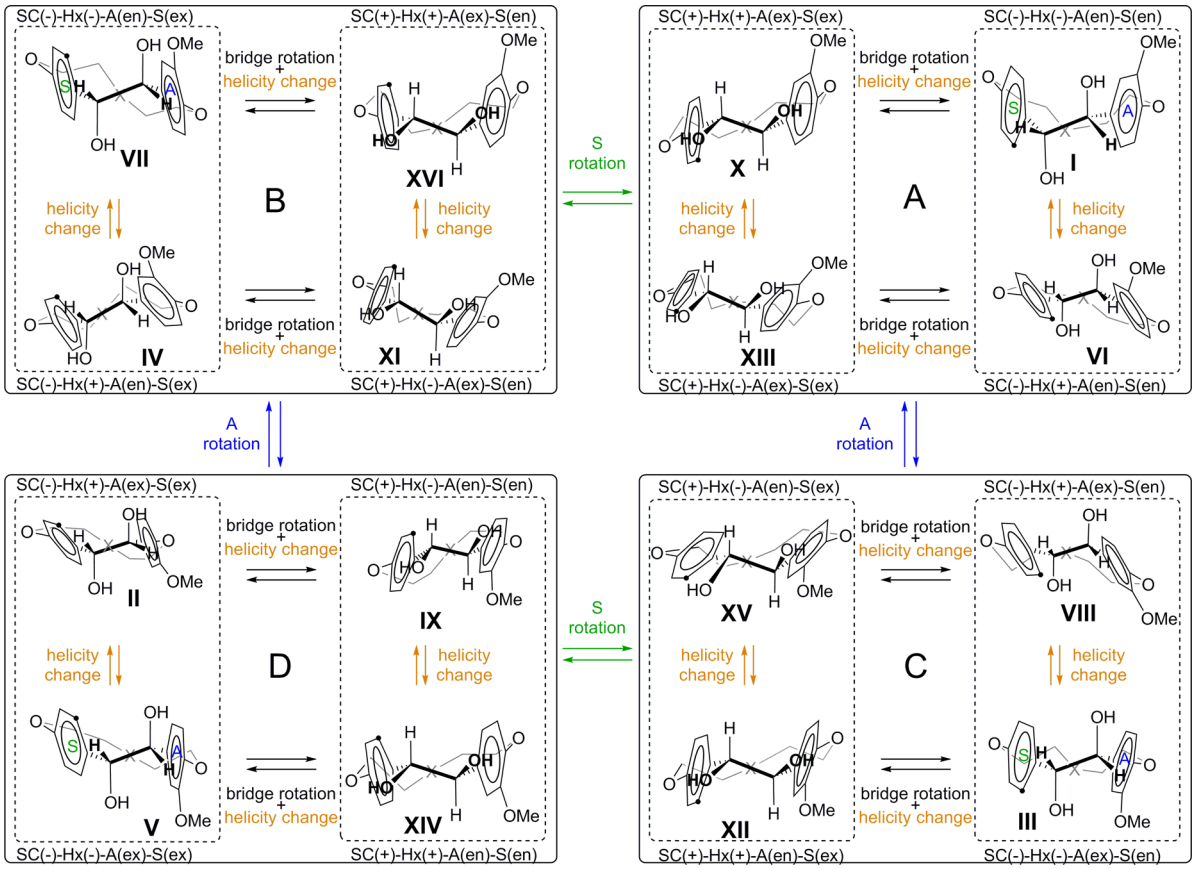

Figure 4. Conformational equilibria of *trans*-diols **5** (X = O) and **6** (X = CH_2CH_2). Due to symmetry, conformation groups A = B and conformation group C = D. Key: SC, synclinal (+ or −); Hx, helicity (+ or −); A, asymmetric ring; S, symmetric ring (*endo* or *exo*, disposition of −OMe in A-ring or marked position in S-ring, as defined in Figure 3). Similar equilibria can be depicted for **2** (X = O, S ring: tetrasubstituted di-OMe-phenyl).

easier changes of helicity often follow other motions with higher rotation barriers, such as bridge and ring rotations. Bridge rotations are characterized by the change of the sign of the dihedral angle of the central bond of the bridge, whereas ring rotations (requiring the pass of the ring plane through the intraanular space) are characterized by the change of their substituents from an *endo*-orientation (toward the other ring, RO group in Figure 3, top left representation) to an *exo*-orientation (directed opposite to the other ring, RO group in Figure 3, middle, left, and right representations) and vice versa.

The conformational equilibria for the macrocyclic diols encompass 16 conformational groups (**I**–**XVI**), as depicted in Figure 4 for compounds **5** and **6**. The eight conformations on the sides of Figure 4 (**I**–**VIII**) display *anti* hydroxy groups, whereas the other eight conformations in the center (**IX**–**XVI**) display them *gauche*. The four transitions described in Figure 3 represent the simplest paths for the exchange between the conformations. Framed groups of four conformations (quartets A, B, C, and D) do not need ring rotations to exchange within, while switching frames requires ring rotation(s). In every figure, the quartets have been placed such that rotations of symmetric S-rings (when present) occur horizontally and rotations of asymmetric A-rings occur vertically. Within each quartet, two dotted frames contain easily exchanging pairs of conformations with different helicity. In turn, exchange between dotted frames is accomplished by bridge rotations (that involve helicity change).

***trans*-Diols.** According to the previous considerations, the conformational equilibrium for diol **5** (and diol **6**, X = CH_2CH_2) is depicted in Figure 4. If the appropriate modifications are introduced it can also be applied to diols **2**, **3**, and **10** and their acetates.

trans-Diols **2**, **3**, **5**, **6**, and **10** have one symmetrical ring, thus making quartet A equal to B and quartet C, equal to D. All of them show in their NMR spectra (^{1}H and ^{13}C, $CDCl_3$, rt) different signals for the chemically equivalent nuclei of the symmetric rings. This later observation indicates that the rings rotate slowly in the NMR time scale. For compounds **2** and **5**, there are two complete sets of signals, whose spectroscopic differences suggest that they differ in the disposition of the substituents on the asymmetric phenyl rings with respect to the macrocyclic intra-annular space (*endo* vs *exo*, Figure 5). Bridge conformations corresponding to *antiperiplanar* hydroxy groups are not observed; thus, under these conditions, they are either below the detection limit of the NMR or rapidly exchanging with the observed ones. This further reduces the eight conformational groups corresponding to two quartets (A = B and C = D), to just the four conformations with synclinal hydroxy groups (X and XIII for A and XII and XV for C). The major conformer corresponds to quartet A/B and the minor one to C/D for **2** (70:30) and **5** (60:40), as shown in Figure 5. Compound **6**, with a longer hexamethylene spacer, shows broadened NMR spectra, which precluded signal assignment, thus suggesting an intermediate exchange in the NMR time scale.

The replacement of the B ring of combretastatin A-4 by an indole (Figure 1) or a 3-substituted indole ring results in highly potent tubulin polymerization inhibitors.[17] This replacement

dx.doi.org/10.1021/jo500798r | J. Org. Chem. 2014, 79, 6840−6857

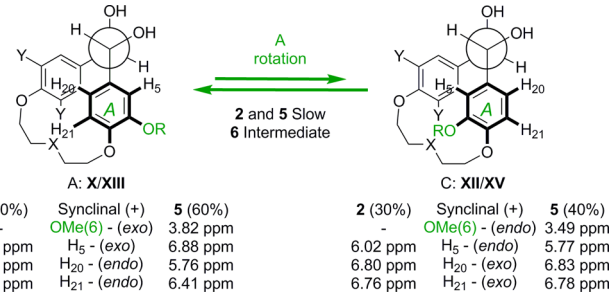

Figure 5. Simplified conformational equilibrium for *trans*-diols **2** (X = O, Y = OMe, R = H; 70%/30%), **5** (X = O, Y = H, R = OMe; 60%/40%) and **6** (X = CH_2CH_2, Y = H, R = Me). (Conformations XI⇆XVI (B) and IX⇆XIV (D) are identical to those in groups A and C, respectively, due to the symmetry of ring S.) Most differing proton chemical shifts for the unsymmetrical A-rings between the two sets of signals observed for compounds **2** and **5** are shown (not for compound **6**, which has broadened NMR spectra). NMR spectra and complete NMR assignments based upon 2D experiments are provided in the Supporting Information.

also results in active macrocyclic combretastatin A analogues.[9] The full conformational equilibria for indolic macrocycles *trans* **8**, **8a**, **10**, and **10a** can be represented as that depicted for **5** and **6** in Figure 4 (see Supporting Information).

The indole ring introduces additional rigidity in the system, as the first carbon atom of the spacer must stay in the plane of the indole. The extra rigidity introduced by the indole results in NMR spectra for compound **10** with a single species at room temperature (Figure 6), with bridge proton signals in

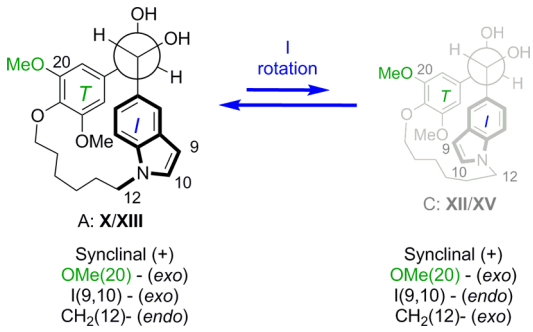

Figure 6. Simplified conformational equilibria for *trans*-diol **10**. Unobserved species are shown reduced and in gray.

agreement with gauche hydroxy groups and the methylene group of the spacer bound to the indole nitrogen (CH_2-12) adopting an *endo* disposition (note that I (*exo*) in Figure 6 refers to the pyrrole methines 9 and 10). Rotation of the symmetric ring (labeled S- or T-tetrasubstituted) is not allowed as it requires the pass of one methoxy group across the intra-annular space, and therefore, exchange of chemically identical groups (A: I–VI–X–XIII to B: IV–VII–XI–XVI, or vice versa, or C: III–VIII–XII–XV to D: II–V–IX–XIV, or vice versa, see Figure 4 and the Supporting Information) does not occur.

Conformations **I–XVI** are all different for compounds **8** and **8a** because both rings (I, indole, and T, trisubstituted) are asymmetric. In consequence, conformational groups A–D are all different. The NMR spectra of diacetate **8a** present two complete sets of signals in slow exchange which were assigned to the *exo*-MeO and the *endo*-MeO conformational groups A and B (Figure 7), as conformations with two axial acetoxy

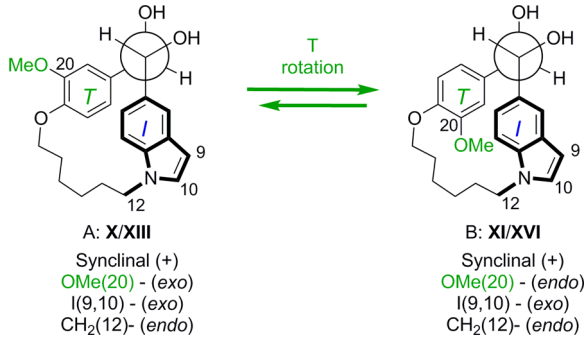

Figure 7. Simplified conformational equilibrium for diol **8** (diacetate **8a**). Observed conformations are X/XIII with *exo*-MeO– and XI/XVI with *endo*-MeO–.

groups are less stable. In the NMR spectra for diol **8**, the signals of the Ph-OMe system (T-ring) are missing due to severe line broadening caused by chemical exchange.

***Trans* Isomers. Solvent Effects and Variable-Temperature Studies.** In order to understand the conformational equilibria in depth, variable-temperature studies were carried out in CD_3OD (from 323 to 213 K) and DMSO-d_6 (from 293 to 353 K). Significant differences were observed between spectra in $CDCl_3$ and in the other solvents or upon temperature changes which are summarized in Table 3. These changes affect the ratio of the conformations in equilibrium and also the number of observed conformations. The most apparent change is the appearance of minor conformations with *gauche* bridge protons and *antiperiplanar* hydroxy groups (**I–VIII**) characterized by smaller coupling constant values between H-2 and H-3 (J < 6 Hz) and a downfield shift from ca. 4.3–4.5 ppm to 4.7–4.9 ppm. We attribute this solvent effect to the relative energetic importance of the intramolecular hydrogen bonds between the two hydroxy groups on the bridge, which cannot form when both hydroxy groups are *anti* to each other. In a low polarity solvent such as $CDCl_3$ the intramolecular hydrogen bond becomes of utmost importance, while in polar, strong hydrogen bond-forming solvents such as CD_3OD or DMSO-d_6 the intermolecular hydrogen bonds with solvent molecules efficiently compete with the intramolecular ones, thus reducing the energetic differences between gauche (**IX–XVI**) and antiperiplanar (**I–VIII**) hydroxy groups. This situation is particularly interesting, as it parallels the equilibrium of binding to their target: conformational preference in $CDCl_3$ likely ressembles more closely that adopted in highly hydrophobic pocket of the colchicine binding site of tubulin while DMSO and methanol ressemble the aqueous reaction media. The importance of intramolecular hydrogen bonds in the pharmacokinetics and pharmacodynamics of drugs has been recently reviewed.[18]

Notably and surprisingly, polar solvents completely shift the equilibria for compound **2** toward the *endo* OH conformations, both in the major (H,H-*anti*, J > 6 Hz) and the minor (H,H-*gauche*, J < 6 Hz) conformations, as deduced from shifts of the H-5, H-20, and H-21 protons in the ^{1}H NMR (Supporting Information). This represents a major conformational shift from **A:X/XIII** (70%) and **C:XII/XV** (30%) in $CDCl_3$ (Figure 5) to **A:I/VI** (15%) and **C:XII/XV** (85%) (Figure 8A). The deshielding of the aromatic protons caused by the nearby bridge hydroxy groups fully agrees with the assignment shown in Figure 8B.

dx.doi.org/10.1021/jo500798r | J. Org. Chem. 2014, 79, 6840–6857

Table 3. Observed Species (>5%) in the ^{1}H NMR Spectra of *trans*-Diols 2, 5, 6, 8, and 10[a]

			$CDCl_3$ r.t.		CD_3OD r.t.		CD_3OD low t. (r.t.→213K)		$DMSO\text{-}d_6$ r.t.		DMSO-d_6 (r.t.→373K)	
			endo	exo	endo	exo	endo	exo	endo	exo	endo	exo
2	H,H OH,OH	*anti gauche*	30%	70%	85%	--	85%	--	85%	--	85%	--
	H,H OH,OH	*gauche anti*	--	--	15%	--	15%	--	15%	--	15%	--
5	H,H OH,OH	*anti gauche*	40%	60%	40%	60%	40%	60%	40%	60%	40%	60%
	H,H OH,OH	*gauche anti*	--	--	--	--	--	--	--	--	--	--
6	H,H OH,OH	*anti gauche*	Unclear (broadened spectrum)		Unclear (broadened spectrum)		30%	44%	Unclear (broadened spectrum)		Continuous variation	
	H,H OH,OH	*gauche anti*					10%	16%				
8	H,H OH,OH	*anti gauche*	H,H-*anti* OH,OH-*gauche* T-ring disappears.		Unclear (broadened) Disappearance of signals		50%	35%	50%	35%	Broadened-Coalescence	
	H,H OH,OH	*gauche anti*					15%		15%			
10	H,H OH,OH	*anti gauche*	1 conformation H,H-*anti* OH,OH-*gauche*		1 conformation H,H-*anti* OH,OH-*gauche*		1 conformation H,H-*anti* OH,OH-*gauche*		1 conformation H,H-*anti* OH,OH-*gauche*		1 conformation H,H-*anti* OH,OH-*gauche* Signals broadening >343K	
	H,H OH,OH	*gauche anti*										

[a]*Endo* and *exo* refer to the disposition of the OH group (A ring) in compound **2**, the OMe group (A ring) in compounds **5** and **6**, or the OMe group (T ring) in compound **8**.

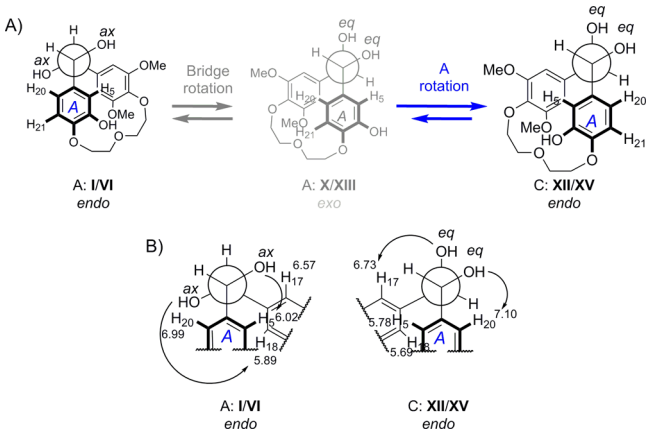

Figure 8. (A) Simplified conformational equilibrium for *trans*-diol **2** in CD_3OD and DMSO-d_6. Minor species are shown in reduced size (left) and not observed species in gray (middle). (B) Deshielding of aromatic protons caused by the nearby bridge hydroxy groups.

In a totally different vein from that described for **2**, diol **5** showed the same conformational distribution, i.e., a 60/40 ratio of the *exo* and *endo* methoxy groups of the A ring with bridge protons always *anti* in either $CDCl_3$, CD_3OD, or DMSO-d_6. Faster exchange upon heating in DMSO-d_6 (343−373 K) results in line broadening and a subtle shift of several signals.

Related diol **6** carrying the hexamethylene spacer shows differences derived from the larger size of the macrocycle (Table 3): (a) the spectra at room temperature in $CDCl_3$, CD_3OD, and DMSO-d_6 correspond with situations of intermediate exchange, where several signals disappear or are broadened, and (b) at lower temperatures, the conformational equilibrium freezes in a mixture of four conformations, two with gauche hydroxy groups (74%) and two with *anti* hydroxy groups (26%). Within each pair, there is a 60:40 ratio of the *endo* and *exo* methoxy groups. Ring rotations and bridge *anti*−*gauche* exchange (synclinarity change) are allowed at room temperature but are all progressively slowed at lower temperatures.

The extra rigidity introduced by the indole and the symmetric ring results in NMR spectra for compound **10** with one major conformation and a very minor one (less than 5%) at room temperature, unappreciable changes in the ^{1}H NMR spectra being observed for compound **10** by changing the solvent, cooling in CD_3OD, or heating in DMSO-d_6.

In the NMR spectra of compound **8** four conformations are observed, which are a consequence of the presence of two asymmetric rings (indole and trisubstituted). At room temperature ($CDCl_3$ and CD_3OD), several signals are missing, probably due to the higher mobility of the T-ring with respect to that of **10** as a result of the removal of one methoxy group. This also results in a general line broadening of the spectra in DMSO-d_6, which shows several conformations at 293 K. As expected, heating in DMSO-d_6 results in coalescence due to the intermediate exchange of the *endo* and *exo* methoxy groups (which are not observed between 323 and 373 K), and cooling below 293 K in CD_3OD differentiates four conformations from 273 to 213 K with only small changes in their shifts. The full conformational equilibria in Figure 9 must be taken into account to include all the species observed for compound **8**. The four observed conformations have *exo* indoles (N−spacer bond *endo*), with *gauche* diols in the major species (upper center) and *anti* diols in the minor ones (lower sides). *Endo* methoxy groups slightly predominate over *exo* ones (Figure 9).

The NMR spectra of *trans*-diols at different temperatures show that subtle structural differences cause changes in the relative stability of the conformations that shift the conformational equilibria from one situation to another, as shown.

***Trans* Isomers. Theoretical Studies.** In order to explore the conformational space accessible to compounds **1**−**10**, we performed Monte Carlo searches using the molecular mechanics MM3 force field with chloroform as implicit solvent.[19] For each compound, any found conformation within 50 kJ/mol of the global minimum was selected, up to 1000. Several dihedral and improper dihedral angles were measured on each conformation and used to classify them in groups labeled **I**−**XVI**, as defined in Figure 4. Most of the found conformations were classified within **I**−**XVI** conformational

dx.doi.org/10.1021/jo500798r | J. Org. Chem. 2014, 79, 6840−6857

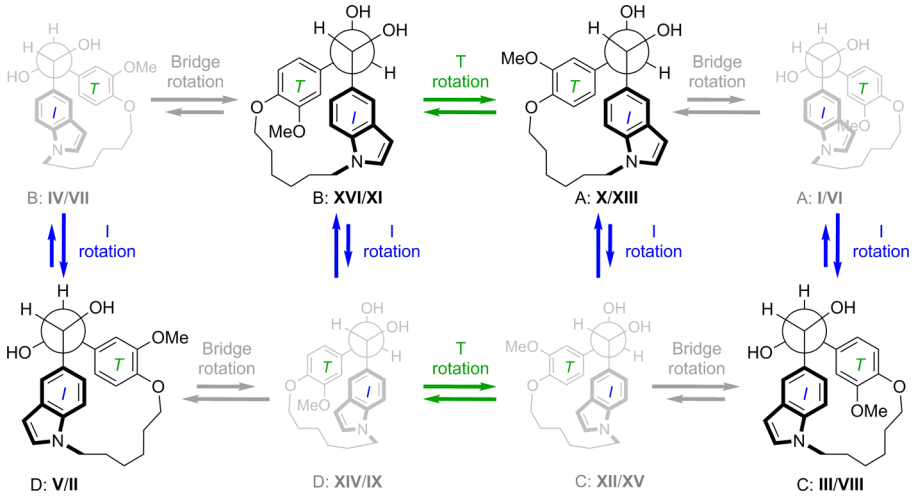

Figure 9. Conformational equilibria of *trans*-diol **8**. As deduced from NMR, conformations XVI (50%), X (35%), and VIII+II (15%) are more stable than I⇆VI (A), IV⇆VII (B), XII⇆XV (C), and IX⇆XIV (D) because of an *endo* N-spacer bond (indole C9,C10 ring-I *exo*).

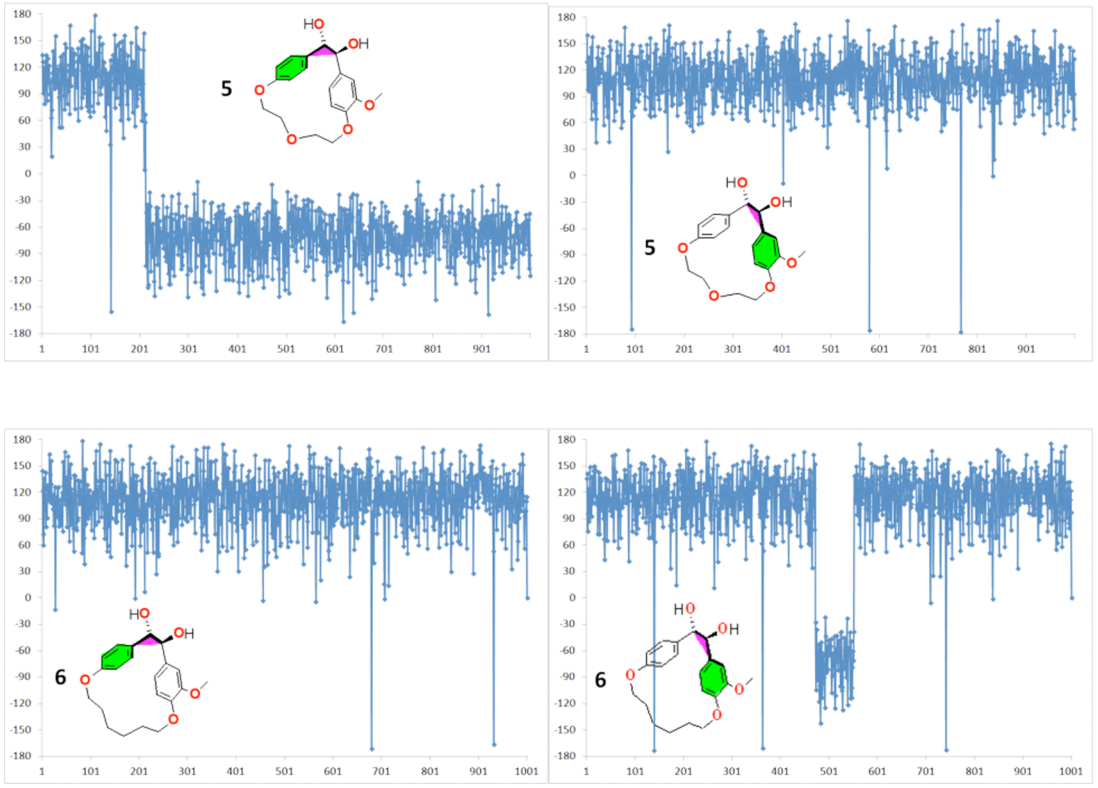

Figure 10. Dihedral angle values for the aromatic rings planes (green plane) and the bridge (pink plane) of **5** and **6** during the 1500 K molecular dynamics simulations.

groups previously described. In most cases, the unclassified conformations were intermediate states between more stable conformations. The global minimum and several of the remaining conformational classes were subsequently used as starting points for the molecular dynamics simulations.

Eight conformations were significantly populated in the conformational searches (Supporting Information, Figure S_MC); four of them are negative bridge synclinals (**I**, **III**, **V**, and **VII**) and four are positive bridge synclinals (**X**, **XII**, **XIV**, and **XVI**). Observed conformations had the same signs of the dihedral angle of the bridge and the dihedral angles of the aromatic ring planes with the bridge (helicity). The structural origin of this preference resides on the spacer: rotating an aromatic ring to adopt a mismatched disposition drives its *endo* side to bump with the spacer, thus making these dispositions less stable. For the *trans*-diols, out of the eight observed conformations, those with synclinal hydroxy groups (**X**, **XII**, **XIV**, and **XVI**) were more stable than those with antiperiplanar (**I**, **III**, **V**, and **VII**). Two factors contribute to this preference: the synclinal hydroxy groups adopt equatorial dispositions and they can form intramolecular hydrogen bonds. Finally, we calculated the relative DFT stabilities of the conformations with a B3LYP-6.31*-SM8 model[20] and observed that they vary within each group of four.

dx.doi.org/10.1021/jo500798r | J. Org. Chem. 2014, 79, 6840−6857

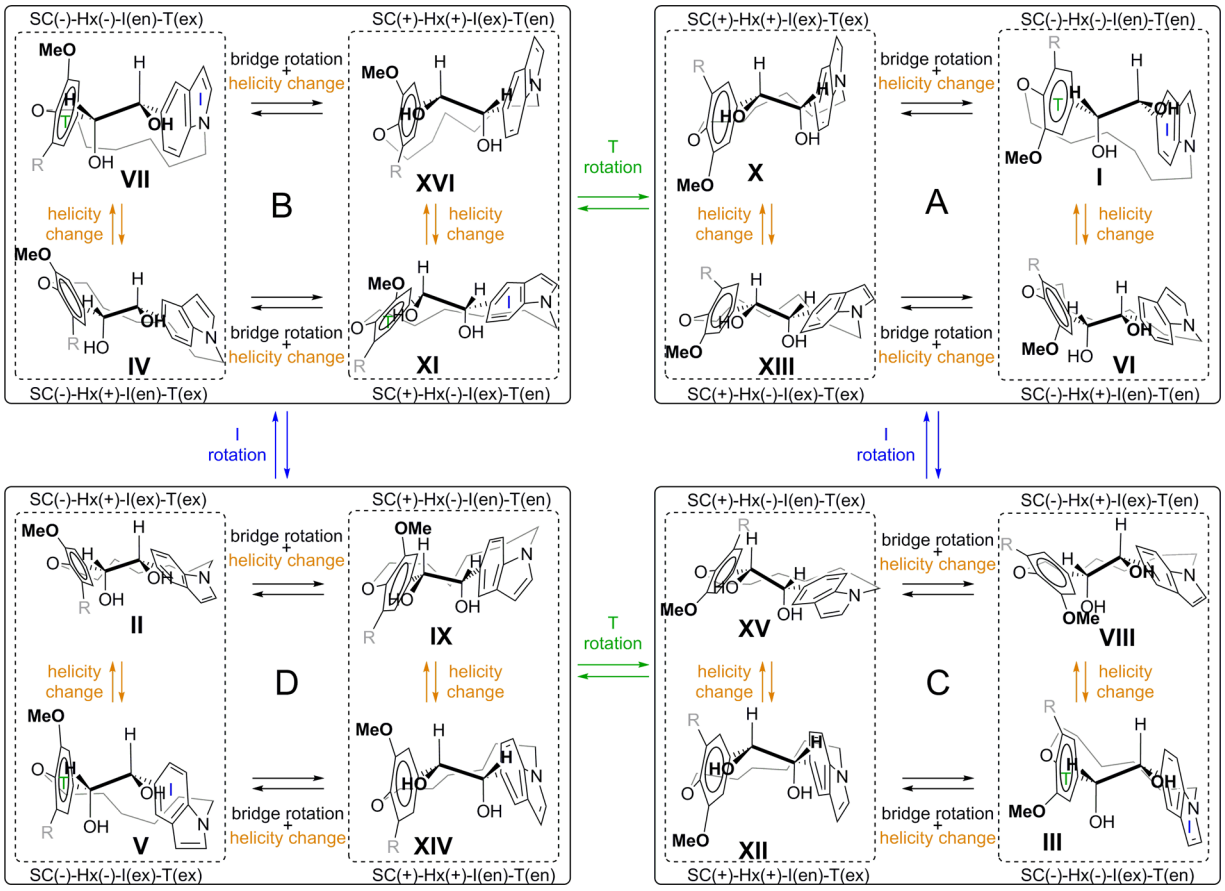

Figure 11. Conformational equilibria of *cis*-diols **7** (R = H) and **9** (R = OMe). Due to symmetry, conformational groups A = B and C = D for compound **9**. Key: SC, synclinal (+ or −); Hx, helicity (+ or −); I, indole ring (indole C9,C10 *exo* or *endo*); T, tetrasubstituted ring in **9**/trisubstituted ring in **7** (*endo* or *exo*, disposition of −OMe).

We next investigated the conformational behavior of these macrocycles by means of molecular dynamics (MD) simulations of 5 ns of length at 300, 600, 1200, and 1500 K. The conformations found along the trajectories were also analyzed and classified in categories **I**−**XVI**. Less than 15% at 300 K and than 25% at 1500 K of the conformations could not be assigned to any of these groups, and they were assigned to a 0 conformational group and subjected to further analysis of their conformational characteristics. Most of them turned out to be conformations in which the two aromatic rings did not have the same sign of the helicity, as previously defined, and the remainder turned out to be conformations in between two conformational classes. These results validate the conformational groups proposed in light of the motions of the bridge and the aromatic rings. Conformations with mismatched signs of the bridge dihedral and aromatic rings planes with the bridge dihedral are populated from the lowest temperature (Supporting Information, Figure S_MD300 K). This suggests that these conformations (**II**, **IV**, **VI**, **VIII**, **IX**, **XI**, **XIII**, and **XV**) are easily accessed despite their higher relative energies. The trajectories were analyzed in search of consecutive conformations belonging to different classes, being the most frequent transitions helicity changes, which usually reverted to the original conformation, followed in frequency by bridge rotations. No ring rotations were observed for any of the compounds at temperatures below 1500 K. This threshold is higher than that previously found by us for related olefins, which display ring rotations at 1200 K, and similar to that found in related diols.[9] Accordingly, below 1500 K (see the Supporting Information, Figure S_MD1200K) the conformations remain within the same conformational group of four (A, B, C, or D) as the initial structure, in good agreement with their being the observed species in the NMR spectra at room and lower temperatures. Conformations with positive bridge synclinals and helicity (**X**, **XII**, **XIV**, and **XVI**) are the most populated and account for the spectral characteristics of the corresponding major species in the NMR spectra. At 1500 K, rotations only occur for rings than can do so by passing unsubstituted ring edges (i.e., aromatic methines) through the intra-annular space, as rings substituted at the two ortho positions of the spacer attachment, such as the tetrasubstituted ring of **2**, **3**, or **10** are not expected to rotate, as this would require the passing of a bulky methoxy group through the intra-anular space. No rotations are observed for **2** and for the indole *trans*-diols **8** or **10**. In the former case, this must be due to the short 3-oxapentamethylene spacer as **3**, just differing in a longer hexamethylene spacer, displays rotations of the phenolic ring. For **5** and **6**, with less substituted phenyl rings, rotations are observed for both phenyl rings (Figure 10). The absence of ring rotations for **8** and **10** can be explained by the additional difficulties imposed by the geometric constraints of the indole ring on the rotation of the other ring, which cause the hexamethylene spacer to behave as if it were shorter. Rotation of the indole itself is also not observed. The difficulty found for bridge and ring rotations in the MD simulations agrees with the observation of several species in the NMR spectra, mainly

dx.doi.org/10.1021/jo500798r | J. Org. Chem. 2014, 79, 6840−6857

corresponding to the two bridge synclinals (the more stable *anti*-H,H being always the major species) combined with the two possibilities (*endo*/*exo*) for the asymmetrically substituted rings (Table 3). NMR spectra at lower temperatures clearly agree with the existence of several nonexchanging species, whose exchange results in the line broadening observed in the NMR spectra upon temperature increases for some of the compounds.

To summarize, the here-described *trans*-diols show conformational equilibria with species presenting *gauche* (at least 75%) and *antiperiplanar* (up to 25%) bridge hydroxy groups. These later minor species were not previously observed in related *trans*-diols with two axially symmetric phenyl rings.[9] Previously, we have considered that gauche and antiperiplanar diols were rapidly exchanging, and therefore, only their average signals were observed. The present results imply a more rigid model where no exchange of the bridge synclinals is observed at room temperature. The ring rotations are still slow in the NMR time scale and allowed us to distinguish the *exo* from the *endo* dispositions of the phenyl ring substituents decorating the macrocycle. Both dispositions are of similar energy, and their ratios do not significantly change in different solvents except for the hydroxy group of **2**, which surprisingly shows an *endo* preference in polar solvents but not in $CDCl_3$.

***cis*-Diols.** Variable-temperature NMR experiments could only be carried out with those obtained in higher yields, i.e. the indolic *cis*-diols **7** and **9**. Sixteen reference conformations depicted in Figure 11 for diols **7** (R = H) and **9** (R = OCH_3) can be considered. All conformations **I**–**XVI** have *gauche* dispositions of the two hydroxy groups and of the two protons, and bridge rotation results in conformations of similar stability as in all cases one hydroxy group is equatorial and the other axial (Table 1). Figure 11 shows conformations **I**–**XVI** in framed groups A–B–C–D of four conformations each exchanging without ring rotations, as explained previously.

The NMR spectra (^1H and ^{13}C, $CDCl_3$, rt) of compound **9** show two complete sets of signals in a 65/35 ratio (60/40 for the diacetate **9a**) with different signals for the chemically equivalent proton pairs of the symmetric tetrasubstituted T-ring. The signals of both conformations show little differences consistent with a similar disposition of the rings (*exo* indole), and with a slow exchange between the two *gauche* bridge dispositions (Figure 12). The more remarkable differences can be explained by the deshielding effect of each bridge hydroxy group on the nearby *ortho* proton of the vicinal aromatic ring.

Taking into account that groups A = B and C = D for diol **9**, the conformational equilibrium in Figure 11 can be summarized as shown in Figure 13 for one enantiomer: conformations with a (−)-synclinal bridge are preferred (**III**, major on the right,

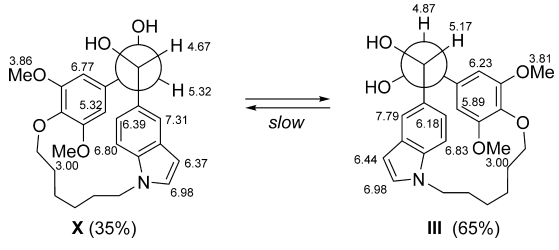

X (35%) **III** (65%)

Figure 12. Conformational equilibrium of *cis*-diol **9** showing the differences produced by the OHs of the bridge on the nearby protons (H-5, -21, -22, -24).

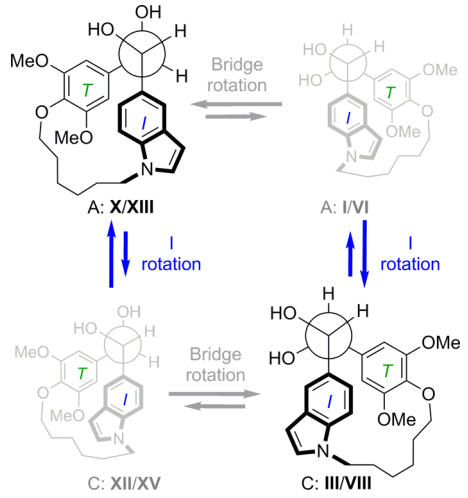

Figure 13. Simplified conformational equilibria of *cis*-diol **9** showing the preference for conformations **X** and **III**.

OH *gauche* to the indole) over those with a (+)-synclinal bridge (**X**, on the left, OH *gauche* to the di-OMe-Ph), *exo* indoles are preferred over *endo* (**X**, **XIII** > **XII**, **XV** and **III**, **VIII** > **I**, **VI**), and conformations with identical sign of *synclinal* and *helicity* are also preferred (**X** > **XIII** and **III** > **VIII**).

7 and its diacetate **7a** show two severely broadened sets of signals at room temperature and some signals do not appear, thus pointing out to a dynamic behavior.

***Cis* Isomers. Solvent Effects and Variable-Temperature Studies.** Variable-temperature studies in CD_3OD (from 323 to 213 K) and DMSO-d_6 (from 293 to 353 K) are shown in Table 4. There are small differences between spectra in these

Table 4. Changes Observed in ^1H NMR Spectra of *cis*-Diols 7 and 9

			$CDCl_3$ r.t.	CD_3OD r.t.	CD_3OD low t. (r.t.→213K)		DMSO-d_6 r.t.	DMSO-d_6 (r.t.→373K)
7			endo/exo	endo/exo	(213→263K)		endo/exo	(293→313K)
					endo	exo		endo/exo
	bridge	(+)-SC	40% br	40% br	22%	21%	40% br	40%
	bridge	(-)-SC	60% br	60% br	44%	13%	60% br	60% br
					(273→293K) endo/exo			(323→343K) Coalescence
	bridge	(+)-SC			40% br			(353→373K) 1 set appearing
	bridge	(-)-SC			60% br			
					(303→323K) Coalescence			
9					(213→293K)			
	bridge	(+)-SC	35% br	35% br	35% br		35% br	35% br
	bridge	(-)-SC	65% br	65% br	65% br		65% br	65% br
					(303→323K) Line broadening			(323→343K) Coalescence
								(353→373K) 1 broad set

solvents at room temperature. For *cis*-diols the strong conformational preference seen in *trans*-diols for one of the bridge synclinals over the other does not occur, thus increasing the number of observed species. As observed for the *trans*-diols, there are no significant changes in the species distribution with temperature, thus suggesting a dominance of the enthalpic term.

For compound **9**, two conformations in an ca. 65/35 ratio are observed in any solvent ($CDCl_3$, CD_3OD, DMSO-d_6) and below 310 K. In DMSO-d_6 at temperatures between 323 and 373 K, exchange becomes faster (**X**⇆**III**), and the signals

dx.doi.org/10.1021/jo500798r | J. Org. Chem. 2014, 79, 6840−6857

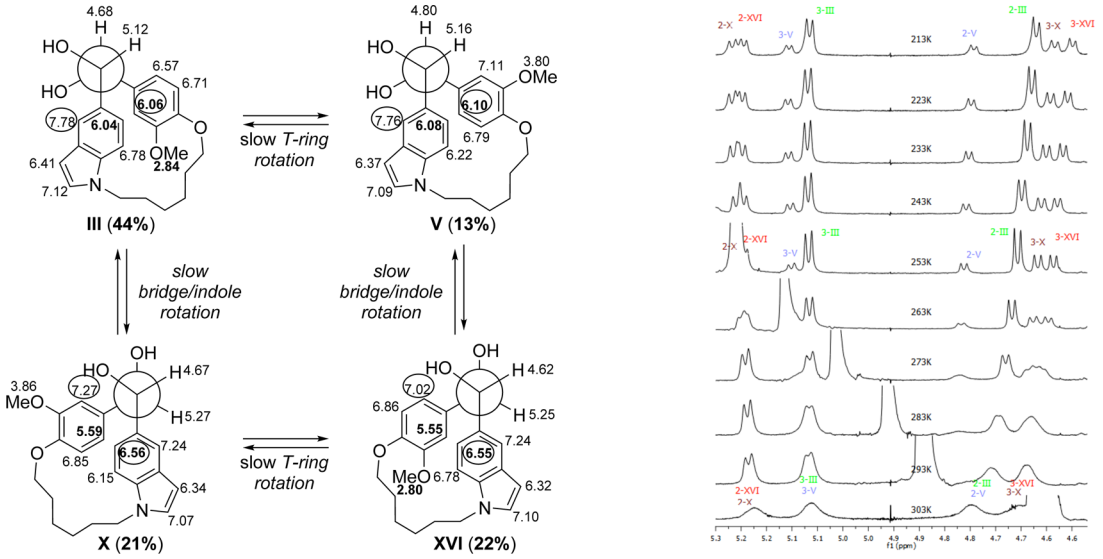

Figure 14. (Left) Observed conformations of compound **7** at low temperature and ^{1}H NMR chemical shifts (273 K, CD_3OD). Encircled aromatic signals are deshielded by the effect of vicinal OH group on the bridge, and bold chemical shifts indicate ring current effects. For selected protons 2, 3, 5, and 24 shifts are comparable for III and V (−synclinal) or X and XVI (+synclinal), whereas for protons 6, 23, and OMe-20 similar surroundings are found in III and XVI (MeO-*endo*) or in V and X (MeO-*exo*). (Right) NMR spectra at different temperatures in the region of the bridge protons H-2 and H-3 showing four conformations (III, V, X, XVI) of compound **7**. Coalescence of signals of conformations III and V and those of conformations X and XVI occurs at 303 K.

broaden and coalesce until at higher temperatures only one averaged set is observed.

The four complete sets of signals for compound **7** at temperatures lower than 273 K (Figure 14) correspond with the four quartets (A–D) represented by their more stable conformations: **X** (A), **XVI** (B), **III** (C), and **V** (D). The relative stabilities of the different conformations can be accounted for in a similar way as for the *trans*-diols: *exo* indoles (C9,C10 *exo*, C11–N *endo*) are preferred over *endo* indoles (A: **X**/**XIII** > **I**/**VI**, B: **XI**/**XVI** > **IV**/**VII**, C: **III**/**VIII** > **XII**/**XV**, D: **II**/**V** > **IX**/**XIV**) and within each of these couples, identical signs of *synclinal* and *helicity* are strongly preferred (A: **X** > **XIII**, B: **XVI** > **XI**, C: **III** > **VIII**, D: **V** > **II**). Among them, those with *endo*-methoxy groups (**III** and **XVI**) are more stable (66% vs 34%) than those with *exo* ones (**X** and **V**).

For **7**, increasing the temperature from 213 to 323 K (in CD_3OD) and from 293 to 373 K (in DMSO-d_6) collapses the signals of the two (−)-*synclinal* conformations (major **III** and minor **V**) on one side and those of the (+)-*synclinal* conformations on the other (intermediate **X** and **XVI**). Both exchange an *endo*-methoxy group (**III** and **XVI**) with the corresponding *exo*-methoxy group (**V** and **X**) involving T-ring rotations. Therefore, this implies that bridge rotation is slower than rotation of the trisubstituted phenyl ring. At higher temperatures, line broadening and coalescence of the signals is observed. Although indole rotations could be easier than T-ring rotations they produce less stable conformations (9,10-indole *endo*, *N*-methylene *exo*).

***Cis* Isomers. Theoretical Studies.** These studies were performed as described above for the *trans* isomers; the results are consistent with those described for the *trans*-diols, and only significant differences will be discussed.

As occurs with the *trans*-diols, rotation of the aromatic rings is only observed at 1500 K in the molecular dynamics simulations, but a trend of easier ring rotation of the *cis*-diols compared to the *trans* is apparent from the MD simulations (e.g., compare the ring rotations for a single MD simulation at 1500 K for *cis*-diol **7** with *trans*-diol **8** in Figure 15). Analysis of the molecular dynamics simulations trajectories and of the DFT calculations of the reaction coordinates indicate that ring rotation occurs with simultaneous bridge rotation. The NMR spectra of diols **7** and **8** in CD_3OD at room temperature and below confirm this trend, as the *trans*-diol shows different signals for the *exo* and *endo* dispositions of the trisubstituted phenyl ring (Table 3), whereas for the *cis*-diol signal averaging is already patent (Table 4), thus evidencing a faster ring rotation. This is confirmed by the freezing of the ring rotations at lower temperatures, which results in four different observable conformations (Table 4 and Figure 14).

In summary, *cis*-diols show conformational equilibria with species presenting positive and negative bridge synclinals. Phenyl rings exchange fast in the NMR time scale, thus presenting averaged resonances which allowed for a straightforward discrimination from their *trans* counterparts. However, introduction of an indole ring results in a slow exchange of the bridge synclinals which results in a more *trans* like chemical shifts of the mutually exchanging resonances of symmetric rings. The ring rotations are also slow in the NMR time scale but they occur more readily than in the *trans* isomers. Theoretical studies suggest that they occur coupled to bridge rotations, which are easier in the *cis* isomers due to the lower energy difference between conformations with opposite signs of the bridge synclinal. The indole rings also restrict the accessible conformations to their *exo* dispositions, because they force the first carbon of the spacer to lie in the same plane as the ring, thus reducing its effective length and the flexibility of the macrocycle.

Tubulin Polymerization Inhibition. The tubulin polymerization inhibitory (TPI) activity of diols **4**–**8** and acetates **7a** and **8a** was evaluated (Table 5) following a previously described protocol[17] and compared with that already described for **1**–**3**, **9**, and **10** and their acetates.[9] The latter group corresponds to combretastatin analogues with three alkoxy substituents on ring A (Figures 1 and 2), whereas in the former

dx.doi.org/10.1021/jo500798r | J. Org. Chem. 2014, 79, 6840–6857

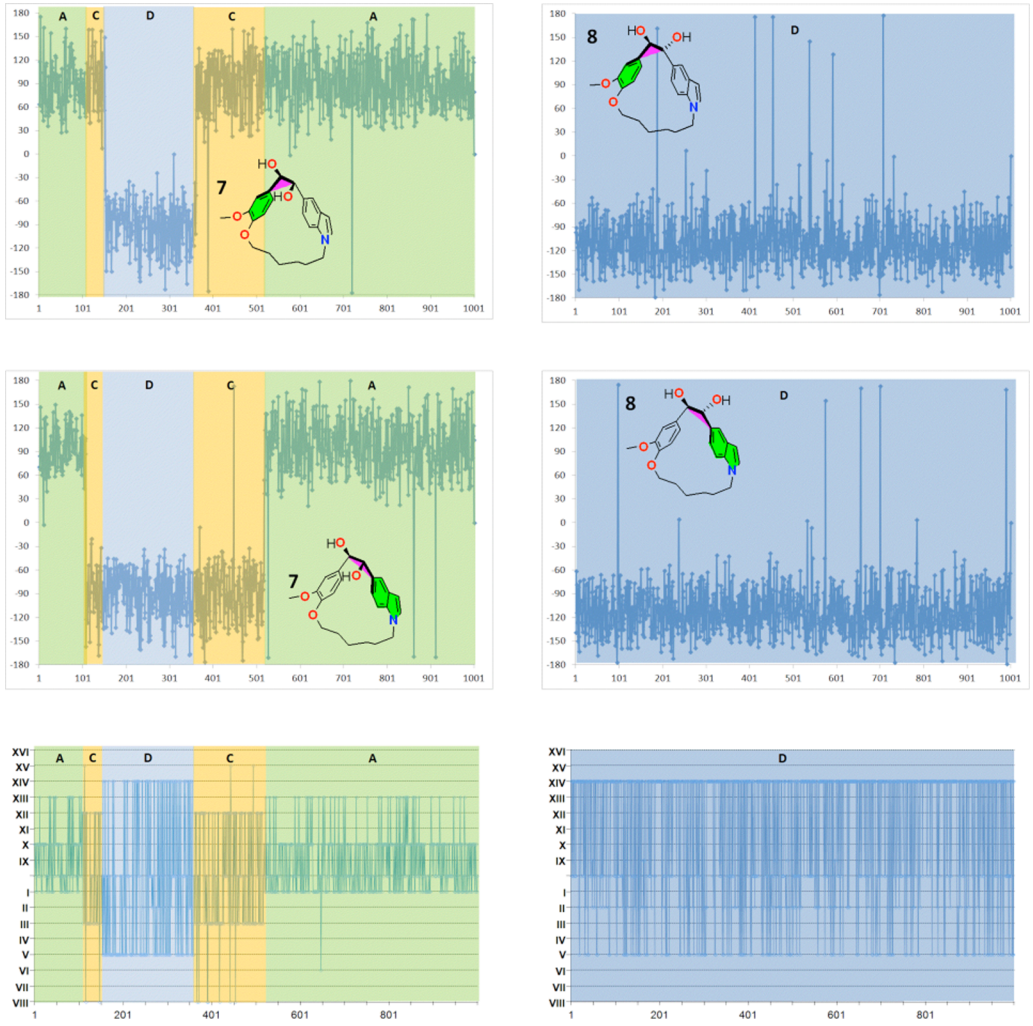

Figure 15. Dihedral angle values for the aromatic rings planes and the bridge (color as in Figure 10) of **7** and **8** during the 1500 K molecular dynamics simulations and conformation class corresponding to each one (time periods corresponding to the A, B, C, and D conformational groups have been uniformly color shaded to illustrate the results of the ring rotations).

group one methoxy group has been removed. Although they are less potent than reference compound CA-4, some considerations can be deduced within this family of macrocyclic analogues.

A trimethoxyphenyl ring (trialkoxy for macrocyclized analogues) is considered essential for TPI activity in combretastatins and related compounds,[21] but macrocycles **4**−**6**, with only two of them on ring A, are the first macrocyclic combretastatins B analogues that are weak inhibitors of tubulin polymerization, and they are more potent than their trialkoxylated A ring analogues. The removal of one methoxy group was an attempt to leave some extra room for the spacer, which would in turn replace it. These diols are less potent than the corresponding macrocyclic olefins with an identical substitution pattern, which shows TPI values of 40−50% at concentrations of 20 μM (compare entries 17, 18, and 20 with entries 16 and 19),[9] but considering that the diols are racemic mixtures of two enantiomers they are comparable. For this substitution pattern on the phenyl rings the nature of the spacer seems to have a small impact on the potency, as diols **5** and **6** (3-oxapentamethylene vs hexamethylene spacer) show similar potency to each other as do their olefins. Indolic diols (entries 22−25 and 27−30) are completely inactive, while their olefins (entries 21 and 26) are among the most potent of their class. This potency fall must be due to conformational issues exclusive to the indolic macrocycles, as the ring substitution patterns give active olefins and the dihydroxylated bridges can occur in active compounds, such as **5** and **6**.

The aromatic rings of the macrocyclic diols present high structural similarity with those of combretastatin A-4 (CA-4, Figure 1) and podophyllotoxin, and therefore, their relevant conformations for binding to tubulin can be deduced from the disposition of the aromatic rings of podophyllotoxin when in complex with tubulin as determined by X-ray crystallography.[22] In every case, the methoxy-substituted phenyl rings correspond with the pendant E ring of podophyllotoxin (a trimethoxyphenyl ring, referred to as E rings in Figure 16), while the other rings correspond to the benzodioxole (referred to as BD rings in Figure 16). With respect to the BD rings, in non−macrocyclic combretastatins the 3-hydroxy-4-methoxyphenyl group (present in compounds **1**−**3**) or the 4-methoxyphenyl group (present in compounds **4**−**6**) produce similar results of TPI.[7,21] Finally, we have shown that a *N*-methyl-5-indolyl (present in compounds **7**−**10**) is a good replacement for ring B of combretastatins (BD podophyllotoxin), with the additional advantage of easily providing anchor points for further modification.[17]

dx.doi.org/10.1021/jo500798r | J. Org. Chem. 2014, 79, 6840−6857

Table 5. Tubulin Polymerization Inhibitory Activity for Macrocyclic Diols and Acetates 1−10a, Compounds in Ref 9c, and Related Derivatives

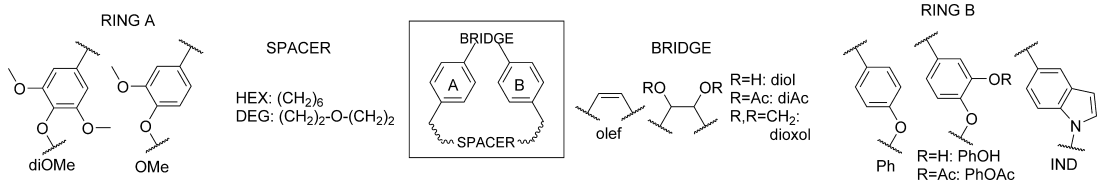

Entry	Spacer	Ring A	Ring B	Bridge	n°	conc uM	% ITP	Entry	Spacer	Ring A	Ring B	Bridge	n°	conc uM	% ITP
1	DEG	diOMe	Ph	olefin	Ref 9c	30	0	16	DEG	OMe	Ph	olefin	olef. of **4-5**	20	44
2	DEG	diOMe	Ph	diol-*cis*	Ref 9c	40	0	17	DEG	OMe	Ph	diol-*cis*	**4**	40	38
3	DEG	diOMe	Ph	diOAc-*trans*	Ref 9c	40	0	18	DEG	OMe	Ph	diol-*trans*	**5**	40	19
4	DEG	diOMe	Ph	diOAc-*cis*	Ref 9c	40	0	19	HEX	OMe	Ph	olef	olef. of **6**	20	48
5	DEG	diOMe	Ph	diOAc-*trans*	Ref 9c	40	0	20	HEX	OMe	Ph	diol-*trans*	**6**	40	26
6	DEG	diOMe	Ph	dioxol-*cis*	Ref 9c	40	0	21	HEX	OMe	IND	olefin	olef. of **7-8**	20	19
7	HEX	diOMe	Ph	olef	Ref 9c	40	60	22	HEX	OMe	IND	diol-*cis*	**7**	40	0
8	HEX	diOMe	Ph	diol-*trans*	Ref 9c	40	4	23	HEX	OMe	IND	diOAc-*cis*	**7a**	40	18
9	HEX	diOMe	Ph	diOAc-*trans*	Ref 9c	40	0	24	HEX	OMe	IND	diol-*trans*	**8**	40	0
10	DEG	diOMe	PhOH	diol-*cis*	**1**	40	11	25	HEX	OMe	IND	diOAc-*trans*	**8a**	40	0
11	DEG	diOMe	PhOH	diol-*trans*	**2**	40	1	26	HEX	diOMe	IND	olefin	olef. of **9-10**	20	44
12	DEG	diOMe	PhOAc	diOAc-*cis*	**1a**	40	0	27	HEX	diOMe	IND	diol-*cis*	**9**	20	11
13	DEG	diOMe	PhOAc	diOAc-*trans*	**2a**	40	0	28	HEX	diOMe	IND	diOAc-*cis*	**9a**	20	9
14	HEX	diOMe	PhOH	olefin	olef. of **3**	40	0	29	HEX	diOMe	IND	diol-*trans*	**10**	20	9
15	HEX	diOMe	PhOAc	diOAc-*trans*	**3**	40	2	30	HEX	diOMe	IND	diOAc-*trans*	**10a**	20	8
								31	CA-4					3	50

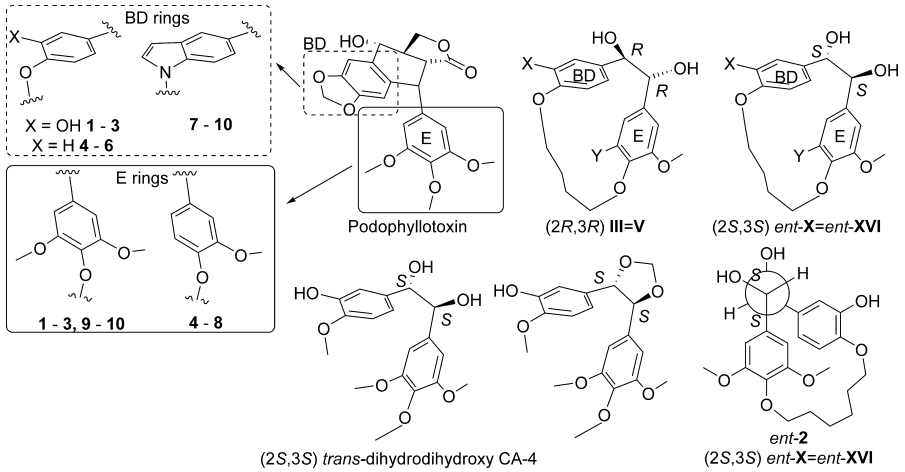

Figure 16. (Top) Schematic drawing of podophyllotoxin when in complex with tubulin and the replacements of the benzodioxole (BD) and trimethoxyphenyl rings (E) found in diols **1−10** and of one conformation of each of the two enantiomers of a generic *trans*-diol which place the phenyl rings in a similar disposition. (Bottom) *S,S*-Diol and dioxolane tubulin polymerization inhibitors with IC_{50} = 14−22 and 4−6 μM, respectively, and Newmann representation of related macrocyclic diol with identical configurations.

The conformation of podophyllotoxin in complex with tubulin puts its phenyl rings in a relative disposition which corresponds to the negative synclinals of the macrocyclic diols, those on the sides of Figures 4 or 11 (*R,R* for *trans* and *R,S* for the *cis*-diols) or the mirror images of the conformations depicted in the center (*trans S,S* and *cis S,R* diols, thereafter referred to as *ent*-conformations).[23] Higher TPI activity has been described for the *S,S* isomer of the *trans*-diol of dihydrodihydroxycombretastatin A-4 and its dioxolane (Figure 16, bottom), thus pointing to a preferred gauche disposition of the hydroxy groups and an important role for an intramolecular hydrogen bond between them.[24]

The superposition of preferred conformations of the diols onto the structure of podophyllotoxin in complex with tubulin (Figure 17) shows a fair structural similarity of the dispositions of their phenyl rings and those of podophyllotoxin, irrespective of their activity in the tubulin polymerization inhibitory assays.[25] For the considered conformations, whatever the relative stereochemistry, intramolecular hydrogen bonds could be formed between the bridge hydroxy groups. The macrocyclization reduces the impact of the intramolecular hydrogen bond on the adoption of the preferred conformation.

With respect to the E rings both *endo* or *exo* dispositions seem in principle equally likely,[26] each forcing the spacer to follow different paths due to steric hindrance: *exo* to the macrocycle for *endo* substituents or *endo* to the macrocycle for *exo* substituents (intermediate if both *endo* and *exo* substituents are present). For BD rings, the spacer can follow two alternative paths as well: one *endo,* toward the side chains of the residues of sheets B8 and B9 (*In*) which in the tubulin−podophyllotoxin complex fill the space between the BD and the E rings and another following the large rim of the podophyllotoxin four ring system (*exo* to the macrocycle),

dx.doi.org/10.1021/jo500798r | J. Org. Chem. 2014, 79, 6840−6857

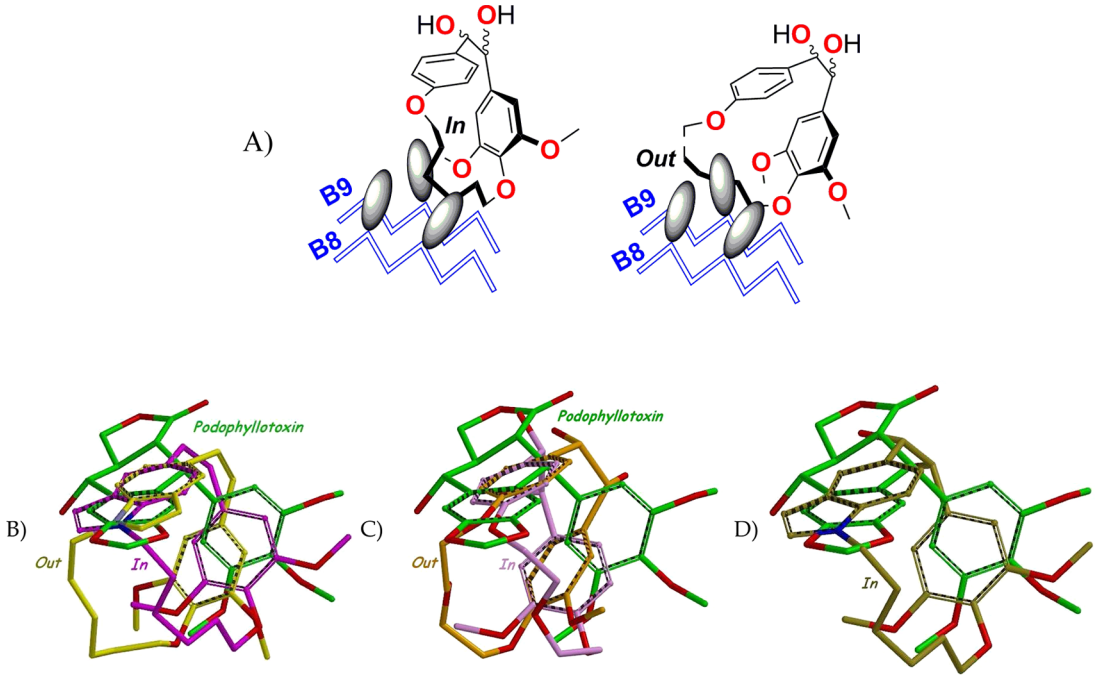

Figure 17. (A) Schematic representation of the binding of macrocyclic diols with the spacer *In* (left), where potential clashes with the side chains (indicated by the gray ellipsoids) of the sheets B8 and B9 of the tubulin structure (represented as zigzag blue lines) arise or *Out* (right) to the macrocycle. Superpositions on the structure of podophyllotoxin (carbons in light green) when in complex with tubulin and (B) the deemed inactive *In* (carbons in magenta) and active *Out* (carbons in yellow) dispositions of the so far most active macrocycle, the indolecombretastatin A; (C) the most active diol, **4** in the deemed inactive *In* (carbons in pink) and active *out* (carbons in orange) dispositions; (D) the macrocyclic diol **9** (carbons in olive) in its only accessible *In* disposition. Hydrogens have been omitted for clarity. (Enlarged images can be seen in the Supporting Information.)

going around the aforementioned side chains (*Out*) (Figure 17).

In $CDCl_3$, we have not found a significant preference for either disposition in the hydroxylated BD rings, but there is a strong preference for the first one in the indolic diols. The hydroxy groups on the BD rings of combretastatin analogues are believed to adopt an *exo* disposition thus forcing the spacer of diols **1**−**3** *endo* to the macrocycle (In) (Figure 17), thus accounting for their potency loss. Finally, the lack of activity observed for the indolic diols can also be accounted for by the strong preference for an *exo* disposition of the methines of the pyrrole ring (and therefore an *endo N*-spacer), caused by the higher conformational rigidity introduced by the indole. The alternative *Out* binding mode is fully compatible with the indolic olefins, as the olefinic bridge does not impart any preference for the *endo*/*exo* rotation of the indoles.[9]

CONCLUSION

The kinematics of a series of new macrocyclic analogues of combretastatins B with two hydroxy groups on the ethane bridge have been studied by means of a combination of variable-temperature NMR studies, molecular dynamics simulations, and DFT theoretical calculations. The relative configuration of the diols, the substitution patterns on the phenyl rings, and the introduction of additional cycles result in different conformational preferences and dynamic behavior of this kind of macrocycles. The tubulin polymerization inhibitory activity was evaluated and found to be similar in potency to that of previously described related macrocyclic olefins but with significant differences in the structural requirements for the activity, and the impact of their conformational equilibria on the activity has been analyzed. An alternative binding mode for the spacer is proposed for these macrocyclic tubulin polymerization inhibitors.

EXPERIMENTAL SECTION

General Techniques. Reagents were used as purchased without further purification. Solvents (THF, DMF, CH_2Cl_2, and toluene) were dried and freshly distilled before use according to literature procedures. Chromatographic separations were performed on silica gel columns by flash (Kieselgel 40, 0.040−0.063) or gravity (Kieselgel 60, 0.063−0.200 mm) chromatography. TLC was performed on precoated silica gel polyester plates (0.25 mm thickness) with fluorescent indicator UV 254 (Polychrom SI F_{254}). Melting points are uncorrected. ^{1}H NMR and ^{13}C NMR spectra were recorded in $CDCl_3$ on 200/50 MHz or on 400/100 MHz spectrometers. Chemical shifts (δ) are given in ppm downfield from tetramethylsilane as internal standard and coupling constants (J values) are in Hertz. IR spectra were run on a Ft-IR instrument in film or BrK Tablets. GC−MS and FABHRMS analyses were carried out at 70 eV. HPLC were run on at least three different columns (5 mm, 4.6 × 150 mm: C_8, C_{18}, and C_F) under following solvent gradients: Flow: 1 mL/min. Time min. (% CH_3CN/H_2O): 1−3 (30/70), 3−15 (ramp), 15− (100/0). Elemental analyses were run on a CHN apparatus.

Starting materials required for the synthesis were prepared as previously described, whereas intermediate dialdehydes were produced by Mitsunobu, phase transfer, or direct alkylations following the procedures described in our previous papers.[9] The McMurry reactions leading to compounds **1**−**10** were fully described in that paper. In this experimental part, the McMurry reactions are briefly described and the full characterizations of hydroxy derivatives **1**−**10** and acetates are included.

General Procedure for McMurry Reactions. A mixture of $TiCl_4$ 98% (5−10 mol/mol of dialdehyde) and Zn (10−20 mol/mol of dialdehyde) in dry THF (20−100 mL/mmol of dialdehyde) was prepared at 0 °C and refluxed for 30 min, and then a solution of dialdehyde in dry THF (20−40 mL/mmol of dialdehyde) was added and maintained at either room temperature or reflux. The reaction was

dx.doi.org/10.1021/jo500798r | J. Org. Chem. 2014, 79, 6840−6857

poured onto a mixture of EtOAc and HCl 2 M, the aqueous layer was extracted, and the combined organic layers were worked up. Products were separated by chromatography (SiO_2, hexane/EtOAc mixtures with 0.1% triethylamine).[9]

Synthesis of Triols 1 and 2. By treatment of corresponding dialdehyde (260 mg, 0.6 mmol) with a mixture of Zn (430 mg, 6.6 mmol) and $TiCl_4$ (0.4 mL, 3.5 mmol) in THF (25 mL) at reflux for 5 h, the crude reaction product (245 mg) was obtained after the described workup. Chromatographic separation afforded **1** (80 mg, 0.21 mmol, 35%) and **2** (88 mg, 0.23 mmol, 39%).

cis-16,19-Dimethoxy-8,11,14-trioxatricyclo[13.2.2.2^{4,7}]henicosa-1(17),4,6,15,18,20-hexaene-2,3,6-triol (1). ^{1}H NMR (400 MHz, $CDCl_3$, 25 °C, TMS): major conformer (55%) δ = 3.35−4.25 (m, 8H; 4 × CH_2), 3.64 (s, 3H; CH_3), 3.68 (s, 3H; CH_3), 4.79 (d, J = 5.1 Hz, 1H), 4.87 (d, J = 5.1 Hz, 1H), 5.78 (bs, 1H), 5.87 (d, J = 1.6, 1H), 5.93 (dd, J = 1.5, 8.3 Hz, 1H), 6.25 (d, J = 1.6 Hz, 1H), 6.58 (d, J = 8.3 Hz, 1H), 6.78 (d, J = 2.0 Hz, 1H) ppm; minor conformer (45%) δ = 3.35−4.25 (m, 8H; 4 × CH_2), 3.61 (s, 3H; CH_3) 3.70 (s, 3H; CH_3) 4.79 (d, J = 5.1 Hz, 1H), 4.88 (d, J = 5.1 Hz, 1H), 5.70 (d, J = 1.6 Hz, 1H), 5.84 (bs, 1H), 6.22 (d, J = 2.0 Hz, 1H), 6.39 (d, J = 1.6 Hz, 1H), 6.47 (dd, J = 2.0, 8.5 Hz, 1H), 6.68 (d, J = 8.5 Hz, 1H) ppm. ^{13}C NMR (100.6 MHz, $CDCl_3$, 25 °C, TMS): major conformer δ = 55.5 (CH_3), 56.5 (CH_3), 70.0 (CH_2), 72.1 (CH_2), 73.0 (CH_2), 73.5 (CH_2), 75.6 (CH), 75.7 (CH), 102.5 (CH), 103.4 (CH), 113.0 (CH), 114.3 (CH), 118.5 (CH), 133.4 (C), 135.3 (C), 137.0 (C), 145.9 (C), 146.1 (C), 151.4 (C), 152.8 (C) ppm; minor conformer δ = 55.6 (CH_3), 55.7 (CH_3), 70.2 (CH_2), 71.9 (CH_2), 72.3 (CH_2), 72.9 (CH_2), 75.2 (CH), 76.0 (CH), 102.2 (CH), 103.9 (CH), 114.0 (CH), 115.7 (CH), 117.2 (CH), 133.7 (C), 135.6 (C), 137.0 (C), 145.4 (C), 146.0 (C), 151.3 (C), 152.2 (C) ppm. IR (film): λ_{max} = 3390, 1593, 1506, 1125 cm^{-1}. HRMS (TOF): m/z calcd for $C_{20}H_{24}O_8$ + Na^+ 415.1369 [M + Na^+], found 415.1391. HPLC (t_R min): C_8 (8.35), C_{18} (8.96), and $C_{phenylic}$ (7.97). Anal. Calcd for $C_{20}H_{24}O_8$: C, 61.22; H, 6.16. Found: C, 61.43; H, 6.19.

trans-16,19-Dimethoxy-8,11,14-trioxatricyclo[13.2.2.2^{4,7}]-henicosa-1(17),4,6,15,18,20-hexaene-2,3,6-triol (2). ^{1}H NMR (400 MHz, $CDCl_3$, 25 °C, TMS): major conformer (70%) δ = 3.49 (s, 3H, CH_3), 3.50−3.95 (m, 4H), 3.83 (s, 3H, CH_3), 4.09 (bd, J = 11.8 Hz, 1H), 4.35 (m 2H), 4.45 (m, 1H), 4.46 (d, J = 7.4 Hz, 1H), 4.51 (d, J = 7.4 Hz, 1H), 5.49 (bs, 1H), 5.57 (bs, 1H), 5.76 (bd, J = 8.4 Hz, 1H), 6.54 (bs, 1H), 6.57 (d, J = 8.4 Hz, 1H), 6.91 (bs, 1H) ppm; minor conformer (30%) δ = 3.34 (bd, J = 6.8 Hz, 1H), 3.35 (bd, J = 6.8 Hz, 1H), 3.36 (bd, J = 6.8 Hz, 1H), 3.50−3.95 (m, 3H), 3.55 (s, 3H, CH_3), 3.8 (m, 1H), 3.85 (s, 3H, CH_3), 4.36 (bd, J = 12.2 Hz, 1H), 4.52 (d, J = 6.7 Hz, 1H), 4.58 (d, J = 6.7 Hz, 1H), 5.64 (bs, 1H), 5.94 (bs, 1H), 6.02 (bs, 1H), 6.55 (bs, 1H), 6.76 (d, J = 8.1 Hz, 1H), 6.80 (bd, J = 8.1 Hz, 1H). ^{13}C NMR (100.8 MHz, $CDCl_3$, 25 °C, TMS): major conformer δ = 55.2 (CH_3), 56.1 (CH_3), 67.2 (CH_2), 70.9−73.7 × 3 (CH_2), 81.6 (CH), 82.3 (CH), 101.4 (CH), 105.1 (CH), 110.8 (CH), 112.3 (CH), 119.6 (CH), 132.6 (C), 135.5 (C), 137.1 (C), 144.7 (C), 145.0 (C), 152.4 (C), 152.4 (C) ppm; minor conformer δ = 55.6 (CH_3), 56.1 (CH_3), 70.9−73.7 x3 (CH_2), 74.3 (CH_2), 81.6 (CH), 82.4 (CH), 102.4 (CH), 106.5 (CH), 117.0 (CH), 117.8 (CH), 119.4 (CH), 135.7 (C), 135.9 (C), 137.9 (C), 147.4 (C), 148.3 (C), 151.8 (C), 152.4 (C) ppm. IR (film): λ_{max} = 3400, 1593, 1506, 1123 cm^{-1}. HRMS (TOF): m/z calcd for $C_{20}H_{24}O_8$ + Na^+ 415.1369 [M + Na^+], found 415.1398. HPLC (t_R min): C_8 (7.83), C_{18} (8.30), and $C_{phenylic}$ (7.96). Anal. Calcd for $C_{20}H_{24}O_8$: C, 61.22; H, 6.16. Found: C, 61.38; H, 6.22.

Synthesis of *trans*+*cis*-17,20-Dimethoxy-8,15-dioxatricyclo-[14.2.2.2^{4,7}]docosa-1(18),4,6,16,19,21-hexaene-2,3,6-triols. By treatment of 4-((6-(4-formyl-2-hydroxyphenoxy)hexyl)oxy)-3,5-dimethoxybenzaldehyde (315 mg, 0.8 mmol) with a mixture of Zn (523 mg, 8.0 mmol) and $TiCl_4$ (0.5 mL, 4.4 mmol) in THF (25 mL) at 0 C, for 5 h, crude reaction product (370 mg) was obtained after the described workup. The mixture could no be separated by chromatography. Acetylation and chromatography yielded triacetate **3**, as described further.

Synthesis of Diols 4 and 5 and Corresponding Olefin. By treatment of adequate dialdehyde (640 mg, 1.86 mmol) with a mixture of Zn (3820 mg, 58.4 mmol) and $TiCl_4$ (2.0 mL, 18.2 mmol) in THF (300 mL) at reflux for 24 h, crude reaction product (580 mg) was obtained after described workup. Chromatographic separation afforded olefin[9a] (87 mg, 0.28 mmol, 15%), **4** (102 mg, 0.29 mmol, 16%9), and **5** (214 mg, 0.62 mmol, 33%).

cis-6-Methoxy-8,11,14-trioxatricyclo[13.2.2.2^{4,7}]henicosa-1-(17),4,6,15,18,20-hexaene-2,3-diol (4). ^{1}H NMR (400 MHz, $CDCl_3$, 25 °C, TMS): one conformer δ = 3.4−3.6 (m, 4H), 3.45 (s, 3H, CH_3), 4.0−4.2 (m, 4H), 4.86 (m, 1H), 4.90 (d, J = 3.5 Hz, 1H), 6.02 (d, J = 7.9 Hz, 1H), 6.40 (d, J = 8.5 Hz, 1H), 6.5−6.6 (m 1H), 6.5−6.6 (m, 1H), 6.5−6.6 (m, 1H), 6.5−6.6 (m, 1H), 6.94 (d, J = 8.5 Hz, 1H) ppm; another conformer δ = 3.4−3.6 (m, 4H), 3.45 (s, 3H, CH_3), 4.0−4.2 (m, 4H), 4.86 (m, 1H), 4.86 (m, 1H), 6.03 (bs, 1H), 6.38 (d, J = 8.5 Hz, 1H), 6.5−6.6 (m, 1H), 6.5−6.6 (m, 1H), 6.67 (d, J = 8.0 Hz, 1H), 6.73 (d, J = 7.6 Hz, 1H), 6.96 (d, J = 8.5 Hz, 1H) ppm. ^{13}C NMR (100.8 MHz, $CDCl_3$, 25 °C, TMS): one conformer δ = 55.4 (CH_3), 72.2 (CH_2), 67.9 (CH_2), 70.8 (CH_2), 72.8 (CH_2), 75.6 (CH), 75.8 (CH), 109.1 (CH), 114.2 (CH), 118.0 (CH), 115.9 (CH), 118.8 (CH), 127.2 (CH), 125.8 (CH), 131.9 (C), 134.8 (C), 147.9 (C), 150.7 (C), 158.1 (C) ppm; another conformer δ = 55.6 (CH_3), 68.0 (CH_2), 70.0 (CH_2), 72.7 (CH_2), 71.9 (CH_2), 75.5 (CH), 75.7 (CH), 110.4 (CH), 115.0 (CH), 115.4 (CH), 117.9 (CH), 118.8 (CH), 126.4 (CH), 126.9 (CH), 131.9 (C), 134.6 (C), 147.8 (C), 149.7 (C), 159.2 (C) ppm. IR (film): ν_{max} = 3446, 1609, 1511, 1266, 1121 cm^{-1}. HRMS (TOF): m/z calcd for $C_{19}H_{22}O_6$ + Na^+ 369.1314 [M + Na^+], found 369.1327. HPLC (t_R min): C_8 (6.72), C_{18} (6.69) and $C_{phenylic}$ (7.38). Anal. Calcd for $C_{19}H_{22}O_6$: C, 65.88; H, 6.40. Found: C, 65.90; H, 6.43.

trans-6-Methoxy-8,11,14-trioxatricyclo[13.2.2.2^{4,7}]henicosa-1-(17),4,6,15,18,20-hexaene-2,3-diol (5). ^{1}H NMR (400 MHz, $CDCl_3$, 25 °C, TMS): major conformer (60%) δ = 3.64−3.55 (m, 4H), 3.82 (s, 3H, CH_3), 4.00−3.95 (m, 2H), 4.34−4.31 (m, 2H), 4.59 (d, J = 7.3 Hz, 1H), 4.61 (d, J = 7.3 Hz, 1H), 5.76 (dd, J = 8.3, 1.8 Hz, 1H), 6.15 (dd, J = 8.4, 2.2 Hz, 1H), 6.41 (d, J = 8.2 Hz, 1H), 6.42 (dd, J = 8.4, 2.6 Hz, 1H), 6.72 (dd, J = 8.5, 2.6 Hz, 1H), 6.88 (d, J = 1.8 Hz, 1H), 7.20 (dd, J = 8.5, 2.2 Hz, 1H) ppm; minor conformer (40%) δ = 3.49 (s, 3H, CH_3), 3.64−3.55 (m, 4H), 4.00−3.95 (m, 2H), 4.34−4.31 (m, 2H), 4.55 (d, J = 6.9 Hz, 1H), 4.63 (d, J = 6.9 Hz, 1H), 5.77 (d, J = 1.8 Hz, 1H), 6.18 (dd, J = 8.6, 2.2 Hz, 1H), 6.53 (dd, J = 8.6, 2.6 Hz, 1H), 6.66 (dd, J = 8.5, 2.7 Hz, 1H), 6.78 (d, J = 8.1 Hz, 1H), 6.83 (dd, J = 8.1, 1.8 Hz, 1H), 7.22 (dd, J = 8.4, 2.2 Hz, 1H) ppm. ^{13}C NMR (100.8 MHz, $CDCl_3$, 25 °C, TMS): major conformer δ = 55.9 (CH_3), 69.0 (CH_2), 69.6 (CH_2), 72.4 (CH_2), 72.5 (CH_2), 81.9 (CH), 82.1 (CH), 108.7 (CH), 114.9 (CH), 116.9 (CH), 117.2 (CH), 120.7 (CH), 126.0 (CH), 128.6 (CH), 133.9 (C), 135.1 (C), 146.9 (C), 149.7 (C), 158.3 (C) ppm; minor conformer δ = 55.0 (CH_3), 67.0 (CH_2), 72.8 (CH_2), 72.9 (CH_2), 74.7 (CH_2), 81.7 (CH), 82.2 (CH), 112.3 (CH), 112.6 (CH), 116.5 (CH), 117.5 (CH), 120.2 (CH), 125.5 (CH), 129.1 (CH), 132.8 (C), 137.1 (C), 148.4 (C), 150.7 (C), 157.6 (C) ppm. IR (film): $\tilde{\nu}_{max}$ = 3440, 1610, 1500, 1255, 1115 cm^{-1}. HRMS (TOF): m/z calcd for $C_{19}H_{22}O_6$ + Na^+ 369.1386 [M + Na^+], found 369.1359. HPLC (t_R min): C_8 (5.17), C_{18} (5.49), and $C_{phenylic}$ (5.95). Anal. Calcd for $C_{19}H_{22}O_6$: C, 65.88; H, 6.40. Found: C, 66.00; H, 6.11.

Synthesis of Diols 6cis + 6 (Table 1, Entry 6). By treatment of the required dialdehyde (62 mg, 0.17 mmol) with a mixture of Zn (343 mg, 5.25 mmol) and $TiCl_4$ (0.20 mL, 1.77 mmol) in THF (100 mL) at room temperature for 24 h, the crude reaction product (57 mg) was obtained after described workup. Chromatographic separation afforded a 35/65 mixture of **6cis** + **6** (27 mg, 0.075 mmol, 43%).

cis-6-methoxy-8,15-dioxatricyclo[14.2.2.2^{4,7}]docosa-1-(18),4,6,16,19,21-hexaene-2,3-diol (**6cis**) + (*trans*)-6-Methoxy-8,15-dioxatricyclo[14.2.2.2^{4,7}]docosa-1(18),4,6,16,19,21-hexaene-2,3-diol (**6**). Observed signals in the broadened NMR spectra of the mixture. ^{1}H NMR (400 MHz, $CDCl_3$, 25 °C, TMS): observed for major *trans* isomer δ = 4.58 (bs, 2H), 6.5−6.9 (m, 7H), 3.4−4.1 (m, 4H), 1.2−1.6 (m, 8H), 3.73 (s, 3H, CH_3). Observed for minor *cis* isomer δ = 4.93 (d, J = 4.2 Hz, 1H), 4.95 (d, J = 4.2 Hz, 1H) ppm. ^{13}C NMR (100.8 MHz, $CDCl_3$, 25 °C, TMS): observed for major *trans* isomer δ = 132.5 (C), 80.9 (CH), 81.1 (CH), 133.4 (C), 150.5 (C), 145.9 (C), 26.3

dx.doi.org/10.1021/jo500798r | J. Org. Chem. 2014, 79, 6840−6857

(CH_2), 23.6 (CH_2), 23.5 (CH_2), 26.1 (CH_2), 157.0 (C), 55.8 (CH_3) ppm. IR (film): λ_{max} = 3405, 1608, 1511, 1261, 1230, 1136 cm^{-1}. HRMS (TOF): m/z calcd for $C_{21}H_{26}O_5$ + Na^+ 381.1672 [M + Na^+], found 381.1680. HPLC (t_R min): C_8 (11.00), C_{18} (11.33), and $C_{phenylic}$ (10.21). Anal. Calcd for $C_{21}H_{26}O_5$: C, 70.37; H, 7.31. Found: C, 70.60; H, 7.09.

Synthesis of Diols 7 and 8 and Corresponding Olefin. By treatment of the required dialdehyde (1660 mg, 4.54 mmol) with a mixture of Zn (6430 mg, 96.8 mmol) and $TiCl_4$ (5.3 mL, 47.1 mmol) in THF (300 mL) at reflux for 5 h, crude reaction product (1610 mg) was obtained after described workup. Chromatographic separation afforded olefin[9a] (158 mg, 0.46 mmol, 10.1%), **7** (362 mg, 0.95 mmol, 20.9%), and **8** (462 mg, 1.21 mmol, 26.6%).

*cis-20-Methoxy-18-oxa-11-azatetracyclo[17.2.2.1^{4,8}.0^{7,11}]-tetracosa-1(21),4(24),5,7,9,19,22-heptaene-2,3-diol (**7**).* Observed signals in the broadened ^{1}H NMR spectrum (400 MHz, $CDCl_3$, 25 °C, TMS): observed for major conformer (60%) δ = 1.1−1.9 (m, 8H), 3.7−4.2 (m, 4H), 4.91 (bd, 1H), 5.25 (bd, 1H), 6.15 (b, 1H), 6.2−6.4 (b, 1H), 6.3−6.5 (b, 1H), 6.77 (bd, 1H), 6.97 (b, 1H), 7.76 (bs, 1H) ppm; observed for minor conformer (40%) δ = 1.1−1.9 (m, 8H), 3.7−4.2 (m, 4H), 4.82 (bd, 1H), 5.36 (bd, 1H), 6.15 (b, 1H), 6.3−6.5 (b, 1H), 6.7−6.8 (b, 1H), 6.77 (bd, 1H), 6.97 (b, 1H), 7.41 (bs, 1H) ppm. No signals were observed in the broadened ^{13}C NMR spectrum (100.8 MHz, $CDCl_3$, 25 °C, TMS). IR (film): $\tilde{\nu}_{max}$ = 3400, 1577, 1126 cm^{-1}. HRMS (TOF): m/z calcd for $C_{23}H_{27}NO_4$ + Na^+ 404.1838 [M + Na^+], found 404.1808. HPLC (t_R min): C_8 (12.75), C_{18} (13.89), and $C_{phenylic}$ (13.00). Anal. Calcd for $C_{23}H_{27}NO_4$: C, 72.42; H, 7.13, N 3.67. Found: C, 72.52; H, 7.23, N 3.29.

*trans-20-Methoxy-18-oxa-11-azatetracyclo[17.2.2.1^{4,8}.0^{7,11}]-tetracosa-1(21),4(24),5,7,9,19,22-heptaene-2,3-diol (**8**).* Observed signals in the broadened ^{1}H NMR spectrum (400 MHz, $CDCl_3$, 25 °C, TMS): 1.1−1.9 (m, 8H), 3.6−4.2 (m, 2H), 3.76 (bs, 3H, CH_3),), 4.10 (m, 2H), 4.66 (d, J = 7.8 Hz, 1H), 4.73 (d, J = 7.8 Hz, 1H), 5.80−6.90 (m, 3H), 6.24 (bd, J = 8.1 Hz, 1H), 6.43 (d, J = 2.7 Hz, 1H), 6.78 (d, J = 8.1 Hz, 1H), 6.98 (d, J = 2.7 Hz, 1H), 7.65 (bs, 1H) ppm. No signals were observed in the broadened ^{13}C NMR spectrum (100.8 MHz, $CDCl_3$, 25 °C, TMS). IR (film): $\tilde{\nu}_{max}$ = 3385, 1555, 1120 cm^{-1}. HRMS (TOF): m/z calcd for $C_{23}H_{27}NO_4$ + Na^+ 404.1838 [M + Na^+], found 404.1822. HPLC (t_R min): C_8 (12.05), C_{18} (13.01), and $C_{phenylic}$ (12.47). Anal. Calcd for $C_{23}H_{27}NO_4$: C, 72.42; H, 7.13; N, 3.67. Found: C, 72.35; H, 7.03; N, 3.41.

Synthesis of Diols 9 and 10 and Corresponding Olefin (Table 1, Entry 9). By treatment of required dialdehyde (570 mg, 1.44 mmol) with a mixture of Zn (2040 mg, 30.7 mmol) and $TiCl_4$ (1.8 mL, 16.3 mmol) in THF (300 mL) at reflux for 5 h, the crude reaction product (680 mg) was obtained after the described workup. Chromatographic separation afforded olefin[9a] (150 mg, 0.43 mmol, 26.7%), **9** (108 mg, 0.26 mmol, 18.2%), and **10** (100 mg, 0.24 mmol, 16.6%).

*cis-20,23-Dimethoxy-18-oxa-11-azatetracyclo[17.2.2.1^{4,8}.0^{7,11}]-tetracosa-1(21),4(24),5,7,9,19,22-heptaene-2,3-diol (**9**).* ^{1}H NMR (400 MHz, $CDCl_3$, 25 °C, TMS): major conformer (65%) δ = 1.1−1.9 (m, 8H), 3.00 (s, 3H, CH_3), 3.45 (m, 1H), 3.81 (s, 3H, CH_3), 3.95 (m, 1H), 4.10 (m, 2H), 4.87 (d, J = 3.8, Hz, 1H), 5.17 (d, J = 3.8, Hz, 1H), 5.89 (bs, 1H), 6.18 (d, J = 8.8 Hz, 1H), 6.23 (bs, 1H), 6.44 (bs, 1H), 6.83 (d, J = 8.8 Hz, 1H), 6.98 (bs, 1H), 7.79 (bs, 1H) ppm; minor conformer (35%) δ = 1.1−1.9 (m 8H), 3.00 (s, 3H, CH_3), 3.45 (m, 1H), 3.86 (s, 3H, CH_3), 3.95 (m, 1H), 4.10 (m, 2H), 4.76 (bs, 1H), 5.31 (bs, 1H), 5.32 (bs, 1H), 6.37 (bs, 1H), 6.39 (d, J = 8.4 Hz, 1H), 6.77 (bs, 1H), 6.80 (d, J = 8.4 Hz, 1H), 6.98 (bs, 1H), 7.31 (bs, 1H) ppm. ^{13}C NMR (100.8 MHz, $CDCl_3$, 25 °C, TMS): major conformer δ = 23.6 (CH_2), 26.9 (CH_2), 28.6 (CH_2), 31.4 (CH_2), 46.2 (CH_2), 54.6 (CH_3), 56.4 (CH_3), 72.2 (CH_2), 74.7 (CH), 77.7 (CH), 101.4 (CH), 102.3 (CH), 102.7 (CH), 108.6 (CH), 118.1 (CH), 121.7 (CH), 128.1 (CH), 128.5 (C), 129.8 (C), 134.5 (C), 136.0 (C), 136.1 (C), 152.3 (C), 152.4 (C) ppm; minor conformer δ = 23.6 (CH_2), 26.9 (CH_2), 28.6 (CH_2), 31.4 (CH_2), 46.2 (CH_2), 54.8 (CH_3), 56.2 (CH_3), 71.9 (CH_2), 75.3 (CH), 77.7 (CH), 100.6 (CH), 103.2 (CH), 105.1 (CH), 109.5 (CH), 119.0 (CH), 124.4 (CH), 128.0 (CH), 129.1 (C), 130.7 (C), 135.1 (C), 135.8 (C), 135.9 (C), 152.0 (C), 152.4 (C) ppm. IR (film): $\tilde{\nu}_{max}$ = 3325, 1580, 1145 cm^{-1}. HRMS (TOF): m/z calcd for $C_{24}H_{29}NO_5$ + Na^+ 434.1943 [M + Na^+], found 434.1928. HPLC (t_R min): C_8 (12.03), C_{18} (13.34), and $C_{phenylic}$ (12.53). Anal. Calcd for $C_{24}H_{29}NO_5$: C, 70.05; H, 7.10; N, 3.40. Found: C, 70.29; H, 7.41; N, 3.13.

*trans-20,23-Dimethoxy-18-oxa-11-azatetracyclo-[17.2.2.1^{4,8}.0^{7,11}]tetracosa-1(21),4(24),5,7,9,19,22-heptaene-2,3-diol (**10**).* ^{1}H NMR (400 MHz, $CDCl_3$, 25 °C, TMS): δ = 1.1−1.9 (m, 8H), 2.97 (s, 3H, CH_3), 3.61 (m, 1H), 3.86 (s, 3H, CH_3), 4.08 (m, 2H), 4.32 (m, 1H), 4.64 (d, J = 8.1 Hz, 1H), 4.71 (d, J = 8.1 Hz, 1H), 5.37 (d, J = 1.6 Hz, 1H), 6.28 (dd, J = 8.4, 1.4 Hz, 1H), 6.44 (d, J = 2.9 Hz, 1H), 6.66 d 1.6, 6.82 (d, J = 8.4 Hz, 1H), 6.99 (d, J = 2.9 Hz, 1H), 7.69 (s, 1H) ppm. ^{13}C NMR (100.8 MHz, $CDCl_3$, 25 °C, TMS) δ = 23.6 (CH_2), 26.7 (CH_2), 28.6 (CH_2), 31.5 (CH_2), 46.2 (CH_2), 54.7 (CH_3), 56.3 (CH_3), 72.2 (CH_2), 82.0 (CH), 82.6 (CH), 101.2 (CH), 102.1 (CH), 105.7 (CH), 109.1 (CH), 117.6 (CH), 122.1 (CH), 128.3 (CH), 128.6 (C), 130.8 (C), 134.9 (C), 136.2 (C), 136.3 (C), 151.3 (C), 153.0 (C) ppm. IR (film): $\tilde{\nu}_{max}$ = 3305, 1565, 1135 cm^{-1}. HRMS (TOF): m/z calcd for $C_{24}H_{29}NO_5$ + Na^+ 434.1943 [M + Na^+], found 434.1949. HPLC (t_R min): C_8 (11.51), C_{18} (12.60), and $C_{phenylic}$ (12.00). Anal. Calcd for $C_{24}H_{29}NO_5$: C, 70.05; H, 7.10; N, 3.40. Found: C, 70.34; H, 7.28; N, 3.19.

General Procedure for Acetylation Reactions. Either isolated alcohols or isomeric mixtures (*cis* + *trans*) were dissolved in pyridine (1 mL/mmol of alcohol) and treated with acetic anhydride (1 mL/mmol of alcohol). After 2 h, the mixture was diluted with ethyl acetate and extracted with 2 M HCl, 5% $NaHCO_3$, and brine. The combined organic layers were dried over anhydrous Na_2SO_4, filtered, and the solvent rotary evaporated. If necessary, the products were separated by chromatography (SiO_2, hexane/ethyl acetate mixtures with 0.1% triethylamine).

Acetylation of Triol 1. Following the general procedure from triol **1** (49 mg, 0.17 mmol), triacetate **1a** (28 mg, 0.06 mmol, 43%) was isolated after chromatography.

*cis-16,19-Dimethoxy-8,11,14-trioxatricyclo[13.2.2.2^{4,7}]henicosa-1(17),4,6,15,18,20-hexaene-2,3,6-triyl Triacetate (**1a**).* ^{1}H NMR (400 MHz, $CDCl_3$, 25 °C, TMS): major conformer (55%) δ = 2.13 (s, 3H, CH_3), 2.29 (s, 3H, CH_3), 2.32 (s, 3H, CH_3), 3.5−4.5 (m, 8H), 3.58 (s, 3H, CH_3), 3.86 (s, 3H, CH_3), 5.82 (d, J = 1.7 Hz, 1H), 5.82 (d, J = 5.0 Hz, 1H), 6.09 (dd, J = 2.0, 8.6 Hz, 1H), 6.30 (d, J = 1.7 Hz, 1H), 6.37 (d, J = 5.0 Hz, 1H), 6.79 (d, J = 8.6 Hz, 1H), 7.11 (d, J = 2.0 Hz, 1H) ppm. ^{1}H NMR (400 MHz, $CDCl_3$, 25 °C, TMS): minor conformer (45%) δ = 2.28 (s, 3H, CH_3), 2.28 (s, 3H, CH_3), 2.61 (s, 3H, CH_3), 3.5−4.5 (m, 8H), 3.57 (s, 3H, CH_3), 3.92 (s, 3H, CH_3), 5.60 (d, J = 1.7 Hz, 1H), 5.66 (d, J = 5.0, 6.38 (d, J = 5.0 Hz, 1H), 6.40 (dd, J = 2.2, 8.8 Hz, 1H), 6.68 (d, J = 1.7 Hz, 1H), 6.79 d, J = 2.2 Hz, 1H), 6.87 (d, J = 8.8 Hz, 1H) ppm. IR (film): $\tilde{\nu}_{max}$ = 1745, 1605, 1590, 1500, 1133 cm^{-1}. HRMS (TOF): m/z calcd for $C_{26}H_{30}O_{11}$ + Na^+ 541.1686 [M + Na^+], found 541.1683. HPLC (t_R min): C_8 (9.46), C_{18} (9.73), and $C_{phenylic}$ (9.12). Anal. Calcd for $C_{26}H_{30}O_{11}$: C, 60.23; H, 5.83. Found: C, 60.06; H, 5.75.

Acetylation of Triol 2. Following the general procedure, from triol **2** (80 mg, 0.21 mmol) triacetate **2a** (42 mg, 0.08 mmol, 40%) was isolated after chromatography.

*trans-16,19-Dimethoxy-8,11,14-trioxatricyclo[13.2.2.2^{4,7}]-henicosa-1(17),4,6,15,18, 20-hexaene-2,3,6-triyl Triacetate (**2a**).* ^{1}H NMR (400 MHz, $CDCl_3$, 25 °C, TMS): δ = 2.13 (s, 3H, CH_3), 2.18 (s, 3H, CH_3), 2.29 (s, 3H, CH_3), 3.48 (dd, J = 8.8, 13.8 Hz, 1H), 3.49−3.47 (m, 1H), 3.58 (s, 3H, CH_3), 3.64 (dd, J = 8.8, 11.4 Hz, 1H), 3.78 (ddd, J = 2.0, 8.8, 11.4 Hz, 1H), 3.89 (s, 3H, CH_3), 3.95 (ddd, J = 2.0, 7.6, 13.4 Hz, 1H), 4.03 (dd, J = 8.8, 13.8 Hz, 1H), 4.30 (ddd, J = 2.0, 4.4, 13.4 Hz, 1H), 4.46 (dd, J = 3.6, 13.8 Hz, 1H), 5.67 (d, J = 8.6 Hz, 1H), 5.7 (d, J = 1.6 Hz, 1H), 5.87 (d, J = 8.6 Hz, 1H), 6.21 (dd, J = 2.0, 8.6 Hz, 1H), 6.50 (d, J = 1.6 Hz, 1H), 6.75 (d, J = 8.6 Hz, 1H), 7.00 (d, J = 2.0 Hz, 1H) ppm. ^{13}C NMR (100.8 MHz, $CDCl_3$, 25 °C, TMS): δ = 20.7 (CH_3), 21.0 (CH_3), 21.1 (CH_3), 55.4 (CH_3), 56.2 (CH_3), 67.4 (CH_2), 73.0 (CH_2), 73.5 (CH_2), 73.6 (CH_2), 78.1 (CH), 79.5 (CH), 101.9 (CH), 106.0 (CH), 114.5 (CH), 119.3 (CH), 126.2 (CH), 128.2 (C), 132.0 (C), 137.7 (C), 139.4 (C), 149.6 (C), 152.6 (C), 153.1 (C), 168.5 (CO), 170.1 (CO), 170.1 (CO) ppm. IR (film):

dx.doi.org/10.1021/jo500798r | J. Org. Chem. 2014, 79, 6840−6857

$\tilde{\nu}_{max}$ = 1744, 1617, 1594, 1509, 1126 cm^{-1}. HRMS (TOF): m/z calcd for $C_{26}H_{30}O_{11}$ + Na^+ 541.1686 [M + Na^+], found 541.1695. HPLC (t_R min): C_8 (9.40), C_{18} (9.73), and $C_{phenylic}$ (9.22). Anal. Calcd for $C_{26}H_{30}O_{11}$: C, 60.23; H, 5.83.Found: C, 60.10; H, 5.85.

Acetylation of 17,20-Dimethoxy-8,15-dioxatricyclo-[14.2.2.2^{4,7}]docosa-1(18),4,6,16,19,21-hexaene-2,3,6-triol Mixture. Following the general procedure, from a mixture of McMurry reaction product previously described (125 mg, 0.31 mmol), triacetate **3** (50 mg, 0.10 mmol, 32%) was isolated after chromatography.

*trans-17,20-Dimethoxy-8,15-dioxatricyclo[14.2.2.2^{4,7}]docosa-1(18),4,6,16,19,21-hexaene-2,3,6-triyl triacetate (**3**).* ^{1}H NMR (400 MHz, $CDCl_3$, 25 °C, TMS): δ = 1.1−1.8 (m, 8H), 3.65 (s, 3H, CH_3), 3.82 (s, 3H, CH_3), 3.8−4.2 (m, 4H), 5.98 (d, J = 7.8 Hz, 1H), 6.00 (d, J = 7.8 Hz, 1H), 6.20 (d, J = 1.8 Hz, 1H), 6.55 (d, J = 1.8 Hz, 1H) ppm. ^{13}C NMR (100.8 MHz, $CDCl_3$, 25 °C, TMS): δ = 21.1 (CH_3), 21.2 (CH_3), 23.7 (CH_3), 25.7 (CH_2), 26.6 (CH_2), 28.5 (CH_2), 29.9 (CH_2), 55.7 (CH_3), 56.2 (CH_3), 64.5 (CH_2), 71.6 (CH_2), 78.3 (CH), 80.6 (CH), 103.6 (CH), 107.9 (CH), 131.3 (C), 135.3 (C), 137.3 (C), 152.4 (C), 153.2 (C), 153.5 (C), 170.3 (CO), 170.3 (CO), 171.1 (CO) ppm. IR (film): $\tilde{\nu}_{max}$ = 1745, 1610, 1600, 1505, 1123 cm^{-1}. HRMS (TOF): m/z calcd for $C_{28}H_{34}O_{10}$ + Na^+ 553.2050 [M + Na^+], found 553.2078. HPLC (t_R min): C_8 (11.34), C_{18} (11.95), and $C_{phenylic}$ (10.99). Anal. Calcd for $C_{28}H_{34}O_{10}$: C, 63.39; H, 6.46. Found: C, 63.21; H, 6.18.

Acetylation of Diol 7. Following the general procedure, from diol **7** (97 mg, 0.25 mmol), diacetate **7a** (86 mg, 0.18 mmol, 73%) was isolated after chromatography.

*cis-20-Methoxy-18-oxa-11-azatetracyclo[17.2.2.1^{4,8}.0^{7,11}]-tetracosa-1(21),4(24),5,7,9,19,22-heptaene-2,3-diyl Diacetate (**7a**).* ^{1}H NMR (400 MHz, $CDCl_3$, 25 °C, TMS): major conformer (55%) δ = 1.1−1.9 (m, 8H), 2.14 (s, 3H, CH_3), 2.30 s (s, 3H, CH_3), 3.6−4.2 (m, 2H), 3.6−4.2 (m, 2H), 3.85 (bs, 3H, CH_3), 5.99 (d, J = 4.5 Hz, 1H), 6.26 (m, 1H), 6.46 (bs, 1H), 6.47 (bs, 1H), 6.60 (d, J = 4.5 Hz, 1H), 6.79−6.85 (m 1H), 6.79−6.85 (m, 1H), 7.00 (bs, 1H), 7.74 (bs, 1H) ppm; minor conformer (45%) δ = 1.1−1.9 (m, 8H), 2.14 (s, 3H, CH_3), 2.32 (s, 3H, CH_3), 3.10 (bs, 1H), 3.6−4.2 (m, 4H), 5.88 (bs, 1H), 5.99 (d, J = 4.5 Hz, 1H), 6.26 (m, 1H), 6.39 (bs, 1H), 6.60 (d, J = 4.5 Hz, 1H), 6.79−6.85 (m, 1H), 6.79−6.85 (m, 1H), 6.98 (bs, 1H), 7.39 (bs, 1H) ppm. ^{13}C NMR (100.8 MHz, $CDCl_3$, 25 °C, TMS): major conformer δ = 21.1 (CH_3), 21.1 (CH_3), 27.6 (CH_2), 27.8 (CH_2), 29.6 (CH_2), 31.8 (CH_2), 46.0 (CH_2), 56.3 (CH_3), 70.2 (CH_2), 73.7 (CH), 77.4 (CH), 101.0 (CH), 108.9 (CH), 109.6 (CH), 118.0 (CH), 118.7 (CH), 119.5 (CH), 122.8 (CH), 127.9 (C), 128.5 (CH), 129.9 (C), 135.6 (C), 170.0 (CO), 171.1 (CO) ppm; minor conformer δ = 21.1 (CH_3), 21.1 (CH_3), 27.6 (CH_2), 27.8 (CH_2), 29.6 (CH_2), 31.8 (CH_2), 46.0 (CH_2), 69.9 (CH_2), 74.5 (CH), 77.0 (CH), 101.2 (CH), 108.6 (CH), 109.6 (CH), 118.0 (CH), 118.6 (CH), 119.3 (CH), 122.8 (CH), 127.9 (C), 128.5 (CH), 129.8 (C), 135.6 (C), 170.0 (CO), 170.0 (CO) ppm. IR (film): $\tilde{\nu}_{max}$ = 1742, 1594, 1266 cm^{-1}. HRMS (TOF): m/z calcd for $C_{27}H_{31}NO_6$ + Na^+ 488.2049 [M + Na^+], found 488.2035. HPLC (t_R min): C_8 (15.14), C_{18} (16.55), and $C_{phenylic}$ (16.03). Anal. Calcd for $C_{27}H_{31}NO_6$: C, 69.66; H, 6.71; N, 3.01. Found: C, 69.85; H, 7.00; N, 2.87.

Acetylation of Diol 8. Following the general procedure, from diol **8** (72 mg, 0.19 mmol), diacetate **8a** (52 mg, 0.11 mmol, 59%) was isolated after chromatography.

*trans-20-Methoxy-18-oxa-11-azatetracyclo[17.2.2.1^{4,8}.0^{7,11}]-tetracosa-1(21),4(24),5,7,9,19,22-heptaene-2,3-diyl Diacetate (**8a**).* ^{1}H NMR (400 MHz, $CDCl_3$, 25 °C, TMS): one conformer (50%) δ = 1.1−1.9 (m, 8H), 2.13 (s, 3H, CH_3), 2.13 (s, 3H, CH_3), 3.6−4.3 (m, 4H), 3.89 (s, 3H, CH_3), 5.93 (bs, 1H), 6.08 (d, J = 7.9 Hz, 1H), 6.27 (d, J = 7.9 Hz, 1H), 6.40 (bd, 1H), 6.48 (d, J = 8.1 Hz, 1H), 6.71 (d, J = 8.4 Hz, 1H), 6.83 (d, J = 8.1 Hz, 1H), 6.84 (dd, J = 8.4, 1.3 Hz, 1H), 6.96 (d, J = 3.0 Hz, 1H), 7.58 (bs, 1H) ppm; another conformer (50%) δ = 1.1−1.9 (m, 8H), 2.04 (s, 3H, CH_3), 2.13 (s, 3H, CH_3), 3.10 (s, 3H, CH_3), 3.6−4.3 (m, 4H), 5.97 (dd, J = 8.4, 1.5 Hz, 1H), 5.99 (d, J = 8.0 Hz, 1H), 6.07 (d, J = 8.0 Hz, 1H), 6.19 (d, J = 8.1 Hz, 1H), 6.40 (bd, 1H), 6.46 (d, J = 8.4 Hz, 1H), 6.79 (d, J = 8.1 Hz, 1H), 6.87 (bs, 1H), 6.90 (d, J = 3.0 Hz, 1H), 7.58 (bs, 1H) ppm. ^{13}C NMR (100.8 MHz, $CDCl_3$, 25 °C, TMS): one conformer δ = 21.2 (CH_3), 21.2 (CH_3), 26.5 (CH_2), 27.9 (CH_2), 29.5 (CH_2), 32.4 (CH_2), 46.1 (CH_2), 55.8 (CH_3), 69.0 (CH_2), 79.2 (CH), 79.5 (CH), 101.1 (CH), 108.9 (CH), 115.6 (CH), 117.9 (CH), 118.4 (CH), 122.4 (CH), 122.9 (CH), 127.5 (C), 128.5 (CH), 128.8 (C), 131.0 (C), 136.2 (C), 148.1 (C), 150.2 (C), 170.0 (CO), 170.4 (CO) ppm; another conformer δ = 21.0 (CH_3), 21.2 (CH_3), 26.5 (CH_2), 27.2 (CH_2), 29.6 (CH_2), 33.5 (CH_2), 46.2 (CH_2), 56.1 (CH_3), 69.8 (CH_2), 78.7 (CH), 79.5 (CH), 101.0 (CH), 109.8 (CH), 113.6 (CH), 118.0 (CH), 118.7 (CH), 120.1 (CH), 122.9 (CH), 127.3 (C), 128.4 (C), 129.1 (CH), 129.7 (C), 135.7 (C), 147.0 (C), 150.5 (C), 170.2 (CO), 170.4 (CO) ppm. IR (film): $\tilde{\nu}_{max}$ = 1740, 1603, 1266 cm^{-1}. HRMS (TOF): m/z calcd for $C_{27}H_{31}NO_6$ + Na^+ 488.2049 [M + Na^+], found 488.2012. HPLC (t_R min): C_8 (14.92), C_{18} (16.22) and $C_{phenylic}$ (15.99). Anal. Calcd for $C_{27}H_{31}NO_6$: C, 69.66; H, 6.71; N, 3.01. Found: C, 69.94; H, 6.98; N, 2.95.

Acetylation of Diol 9. Following the general procedure, from diol **9** (30 mg, 0.07 mmol), diacetate **9a** (11 mg, 0.02 mmol, 32%) was isolated after chromatography.

*cis-20,23-Dimethoxy-18-oxa-11-azatetracyclo[17.2.2.1^{4,8}.0^{7,11}]-tetracosa-1(21),4(24),5,7,9,19,22-heptaene-2,3-diyl Diacetate (**9a**).* ^{1}H NMR (400 MHz, $CDCl_3$, 25 °C, TMS): major conformer (60%) δ = 1.1−1.9 (m, 8H), 2.14 (s, 3H, CH_3), 2.34 (s, 3H, CH_3), 3.00 (s, 3H, CH_3), 3.60 (m 1H), 3.84 (s, 3H, CH_3), 3.90 (m, 1H), 4.10 (m, 2H), 5.70 (bs, 1H), 6.00 (m, 1H), 6.40 (m, 1H), 6.41 (m, 1H), 6.47 (bs, 1H), 6.60 (bs, 1H), 6.83 (m, 1H), 7.00 (bs, 1H), 7.80 (bs, 1H), ppm; minor conformer (40%) δ = 1.1−1.9 (m, 8H), 2.14 (s, 3H, CH_3), 2.31 (s, 3H, CH_3), 3.00 (s, 3H, CH_3), 3.60 (m, 1H), 3.89 (s, 3H, CH_3), 3.90 (m, 1H), 4.10 (m, 2H), 5.45 (bs, 1H), 5.90(m, 1H), 6.30 (bs, 1H), 6.40 (m, 1H), 6.72 (m, 1H), 6.73 (bs, 1H), 6.81 (m, 1H), 7.00 (bs, 1H), 7.43 (bs, 1H), ppm. IR (film): $\tilde{\nu}_{max}$ = 1742, 1589, 1236, 1126 cm^{-1}. HRMS (TOF): m/z calcd for $C_{28}H_{33}NO_7$ + Na^+ 518.2155 [M + Na^+], found 518.2164. HPLC (t_R min): C_8 (14.88), C_{18} (15.88), and $C_{phenylic}$ (15.70). Anal. Calcd for $C_{28}H_{33}NO_7$: C, 67.86; H, 6.71; N, 2.83. Found: C, 68.05; H, 7.02; N, 2.64.

Acetylation of Diol 10. Following the general procedure, from diol **10** (23 mg, 0.06 mmol), diacetate **10a** (9 mg, 0.02 mmol, 30%) was isolated after chromatography.

*trans-20,23-Dimethoxy-18-oxa-11-azatetracyclo-[17.2.2.1^{4,8}.0^{7,11}]tetracosa-1(21),4(24),5,7,9,19,22-heptaene-2,3-diyl Diacetate (**10a**).* ^{1}H NMR (400 MHz, $CDCl_3$, 25 °C, TMS): δ = 1.1−1.9 (m, 8H), 2.14 (s, 3H, CH_3), 2.15 (s, 3H, CH_3), 3.10 (s, 3H, CH_3), 3.62 (m, 1H), 3.86 (s, 3H, CH_3), 3.95−4.15 (m, 2H), 4.21 (m, 1H), 5.67 (d, J = 1.5 Hz, 1H), 5.93 (d, J = 8.8 Hz, 1H), 6.02 (d, J = 8.8 Hz, 1H), 6.42 (d, J = 3.1 Hz, 1H), 6.48 (d, J = 8.5 Hz, 1H), 6.55 (d, J = 1.5 Hz, 1H), 6.87 (d, J = 8.5 Hz, 1H), 6.99 (d, J = 3.1 Hz, 1H), 7.64 (s, 1H) ppm. ^{13}C NMR (100.8 MHz, $CDCl_3$, 25 °C, TMS): δ = 21.1 (CH_3), 21.2 (CH_3), 23.4 (CH_2), 26.3 (CH_2), 28.4 (CH_2), 31.0 (CH_2), 46.1 (CH_2), 54.9 (CH_3), 56.3 (CH_3), 72.2 (CH_2), 79.1 CH), 79.5 (CH), 101.1 (CH), 102.7 (CH), 106.8 (CH), 109.2 (CH), 118.6 (CH), 122.6 (CH), 128.6 (C), 128.7 (CH), 131.4 (C), 136.1 (C), 136.6 (C), 136.7 (C), 151.6 (C), 153.0 (C), 170.2(CO), 170.4 (CO) ppm. IR (film): $\tilde{\nu}_{max}$ = 1738, 1592, 1266 cm^{-1}. HRMS (TOF): m/z calcd for $C_{28}H_{33}NO_7$ + Na^+ 518.2155 [M + Na^+], found 518.2137. HPLC (t_R min): C_8 (15.12), C_{18} (16.29), and $C_{phenylic}$ (15.74). Anal. Calcd for $C_{28}H_{33}NO_7$: C, 67.86; H, 6.71; N, 2.83. Found: C, 68.11; H, 6.99; N, 2.48.

Tubulin Isolation. Calf brain microtubule protein (MTP) was purified by two cycles of temperature-dependent assembly/disassembly, according to the method of Shelanski et al. modified as described.[16] The solution of MTP was stored at −80 °C. Protein concentrations were determined by the method of Bradford by using bovine serum albumin (BSA) as standard. Eight different MTP preparations were used in the tubulin assembly assays.

Tubulin Assembly. In vitro tubulin self-assembly was monitored turbidimetrically at 450 nm by using a thermostated Thermospectronic Helios A spectrophotometer fitted with a circulating water carousel system. The ligands were stored in DMSO at −20 °C and the amount of DMSO in the assays was 4%, which has been reported not to interfere with the assembly process. The increase in turbidity was followed simultaneously in a batch of six cuvettes (containing 1.0 mg

dx.doi.org/10.1021/jo500798r | J. Org. Chem. 2014, 79, 6840−6857

mL^{-1} MTP in 0.1 M MES buffer, 1 mM ethylene glycol tetraacetic acid (EGTA), 1 mM $MgCl_2$, 1 mM, b-ME, 1.5 mM guanosine triphosphate (GTP), pH 6.7, and the measured ligand concentration), with a control (i.e., with no ligand) always being included. The samples were preincubated for 30−60 min at 20 °C to allow binding of the ligand, and were cooled on ice for 10 min. The cuvettes were then placed in the spectrophotometer at 4 °C and the assembly process was then initiated by a shift in the temperature to 37 °C.

■ ASSOCIATED CONTENT

Supporting Information

Conformational analyses, conformational searches, dynamics simulations, and NMR data of compounds **1**−**10**. Variable-temperature ^{1}H NMR spectra and data of selected compounds. HRMS, HPLC, EA, ^{1}H NMR, and ^{13}C NMR spectra of compounds **1**−**10**. This material is available free of charge via the Internet at http://pubs.acs.org.

■ AUTHOR INFORMATION

Corresponding Author

*Tel: 34 923 294528. Fax: 34 923 294515. E-mail: pelaez@usal.es.

Notes

The authors declare no competing financial interest.

■ ACKNOWLEDGMENTS

This work was supported by the University of Salamanca (Plan Propio de Apoyo a la Investigación 2013-ref. KAC8), the Spanish MICINN (SAF 2008-04242), the Consejería de Educación de la Junta de Castilla y León (SA147U13), the Spanish AECID (PCI-Mediterráneo A1/037364/11), and the EU (Structural Funds)

■ REFERENCES

(1) (a) Pinney, K. G.; Jelinek, C.; Edvardsen, K.; Chaplin, D. J.; Pettit, G. R. In *Anticancer Agents from Natural Products: The Discovery and Development of the Combretastatins*, 2nd ed.; Cragg, G. M. L., Kingston, D. G. I., Newman, D. J., Eds.; Taylor & Francis: Boca Raton, 2005; pp 27−64.

(2) (a) Pettit, G. R.; Singh, S. B.; Hamel, E.; Lin, C. M.; Alberts, D. S.; Garcia-Kendall, D. *Experientia* **1989**, *45*, 209−211. (b) Pettit, G. R.; Singh, S. B.; Schmidt, J. M.; Niven, M. L.; Hamel, E.; Lin, C. M. *J. Nat. Prod.* **1988**, *51*, 517−527. (c) Pettit, G. R.; Singh, S. B.; Niven, M. L.; Hamel, E.; Schmidt, J. M. *J. Nat. Prod.* **1987**, *50*, 119−131.

(3) (a) Pettit, G. R.; Singh, S. B.; Niven, M. L. *J. Am. Chem. Soc.* **1988**, *110*, 8539−8540. (b) Singh, S. B.; Pettit, G. R. *J. Org. Chem.* **1990**, *55*, 2797−2800.

(4) (a) Pettit, G. R.; Cragg, G. M.; Herald, D. L.; Schmidt, J. M.; Lahavanija, P. *Can. J. Chem.* **1982**, *60*, 1374−1376. (b) Pettit, G. R.; Cragg, G. M.; Singh, S. B. *J. Nat. Prod.* **1987**, *50*, 386−391.

(5) (a) http://clinicaltrials.gov. (b) Sosa, J. A.; Elisei, R.; Jarzab, B.; Balkissoon, J.; Lu, S. P.; Bal, C.; Marur, S.; Gramza, A.; Ben-Yosef, R.; Gitlitz, B.; Haugen, B. R. M.; Ondrey, F.; Lu, C.; Karandikar, S.; Khuri, F.; Licitra, L.; Remick, S. C. *Thyroid* **2013**, *25*, 224. (c) Patterson, D. M.; Zweifel, M.; Middleton, M. R.; Price, P. M.; Folkes, L. K.; Stratford, M. R.; Ross, P.; Halford, S.; Peters, J.; Balkissoon, J.; Chaplin, D. J.; Padhani, A. R.; Rustin, G. J. *Clin. Cancer Res.* **2012**, *18*, 1415−1425. (d) Nathan, P.; Zweifel, P.; Padhani, A. R.; Koh, D. M.; Ng, M.; Collins, D. J.; Harris, A.; Carden, C.; Smythe, J.; Fisher, N.; Taylor, N. J.; Stirling, J. J.; Lu, S. P.; Leach, M. O.; Rustin, G. J.; Judson, I. *Clin. Cancer Res.* **2012**, *18*, 3428−3439. (e) Zweifel, M.; Jayson, G. C.; Reed, N. S.; Osborne, R.; Hassan, B.; Ledermann, J.; Shreeves, G.; Poupard, L.; Lu, S. P.; Balkissoon, J.; Chaplin, D. J.; Rustin, G. J. *Ann. Oncol.* **2011**, *22*, 2036−2041.

(6) (a) Patterson, D. M.; Zweifel, M.; Middleton, M. R.; Price, P. M.; Folkes, L. K.; Stratford, M. R.; Ross, P.; Halford, S.; Peters, J.; Balkissoon, J.; Chaplin, D. J.; Padhani, A. R.; Rustin, G. J. *Clin. Cancer Res.* **2012**, *18*, 1415−1425. (b) Kanthou, C.; Tozer, G. M. *Blood* **2002**, *99*, 2060−2069.

(7) Tron, G. C.; Pirali, T.; Sorba, G.; Pagliai, F.; Busacca, S.; Genazzani, A. A. *J. Med. Chem.* **2006**, *49*, 3033−3044.

(8) For examples of ring-forming strategies, see: (a) Jedhe, G. S.; Paul, D.; Gonnade, R. G.; Santra, M. K.; Hamel, E.; Nguyen, T. L.; Sanjayan, G. J. *Bioorg. Med. Chem. Lett.* **2013**, *23*, 4680−4684. (b) Romagnoli, R.; Baraldi, P. G.; Salvador, M. K.; Preti, D.; Aghazadeh Tabrizi, M.; Brancale, A.; Fu, J.; Li, K. H.; Zhang, S. Z.; Hamel, E.; Bortolozzi, R.; Basso, G.; Viola, G. *J. Med. Chem.* **2012**, *55*, 475−488. (c) Akselsen, O. W.; Odlo, K.; Cheng, J. J.; Maccari, G.; Botta, M.; Hansen, T. V. *Bioorg. Med. Chem.* **2012**, *20*, 234−242. (d) Theeramunkong, S.; Caldarelli, A.; Massarotti, A.; Aprile, S.; Caprioglio, D.; Zaninetti, R.; Teruggi, A.; Pirali, T.; Grosa, G.; Tron, G. C.; Genazzani, A. A. *J. Med. Chem.* **2011**, *54*, 4977−4986. (e) Romagnoli, R.; Baraldi, P. G.; Cruz-Lopez, O.; Lopez Cara, C.; Carrion, M. D.; Brancale, A.; Hamel, E.; Chen, L.; Bortolozzi, R.; Basso, G.; Viola, G. *J. Med. Chem.* **2010**, *53*, 4248−4258. (f) Schobert, R.; Biersack, B.; Dietrich, A.; Effenberger, K.; Knauer, S.; Mueller, T. *J. Med. Chem.* **2010**, *53*, 6595−6602. (g) Bonezzi, K.; Taraboletti, G.; Borsotti, P.; Bellina, P.; Rossi, R.; Giavazzi, R. *J. Med. Chem.* **2009**, *52*, 7906−7910. (h) Odlo, K.; Hentzen, J.; dit Chabert, J. F.; Ducki, S.; Gani, O. A.; Sylte, I.; Skrede, M.; Florenes, V. A.; Hansen, T. V. *Bioorg. Med. Chem.* **2008**, *16*, 4829−4838. (i) Zhang, Q.; Peng, Y.; Wang, X. I.; Keenan, S. M.; Arora, S.; Welsh, W. J. *J. Med. Chem.* **2007**, *50*, 749−754. (j) Kaffy, J.; Pontikis, R.; Carrez, D.; Croisy, A.; Monneret, C.; Florent, J. C. *Bioorg. Med. Chem.* **2006**, *14*, 4067−4074. (k) Sanchez Maya, A. B.; Pérez-Melero, C.; Salvador, N.; Peláez, R.; Caballero, E.; Medarde, M. *Bioorg. Med. Chem.* **2005**, *13*, 2097−2107. (l) Wang, L.; Woods, K. W.; Li, Q.; Barr, K. J.; McCroskey, R. W.; Hannick, S. M.; Gherke, L.; Credo, R. B.; Hui, Y. H.; Marsh, K.; Warner, R.; Lee, R. Y.; Zielinski-Mozng, N.; Frost, D.; Rosenberg, S. H.; Sham, H. L. *J. Med. Chem.* **2002**, *45*, 1697−1711.

(9) (a) Álvarez, R.; Mateo, C.; López, V.; Medarde, M.; Peláez, R. *Chem.—Eur. J.* **2011**, *13*, 3406−3419. (b) Mateo, C.; López, V.; Medarde, M.; Peláez, R. *Chem.—Eur. J.* **2007**, *13*, 7246−7256. (c) Mateo, C.; Álvarez, R.; Pérez-Melero, C.; Peláez, R.; Medarde, M. *Bioorg. Med. Chem. Lett.* **2007**, *17*, 6316−6320. (d) Mateo, C.; Pérez-Melero, C.; Peláez, R.; Medarde, M. *J. Org. Chem.* **2005**, *70*, 6544−6547.

(10) Cushman, M.; Nagarathnam, D.; Gopal, D.; Chakraborti, A. K.; Lin, C. M.; Hamel, E. *J. Med. Chem.* **1991**, *34*, 2579−2588.

(11) Cushman, M.; Nagarathnam, D.; Gopal, D.; He, H. M.; Lin, C. M.; Hamel, E. *J. Med. Chem.* **1992**, *35*, 2293−2306.

(12) (a) Simoni, D.; Grisolia, G.; Giannini, G.; Roberti, M.; Rondanin, R.; Piccagli, L.; Baruchello, R.; Rossi, M.; Romagnoli, R.; Invidiata, F. P.; Grimaudo, S.; Jung, M. K.; Hamel, E.; Gebbia, N.; Crosta, L.; Abbadessa, V.; Di Cristina, A.; Dusonchet, L.; Meli, M.; Tolomeo, M. *J. Med. Chem.* **2005**, *48*, 723−736. (b) Pettit, G. R.; Lippert, J. W., 3rd; Herald, D. L.; Hamel, E.; Pettit, R. K. *J. Nat. Prod.* **2000**, *63*, 969−974. (c) Pettit, G. R.; Toki, B. E.; Herald, D. L.; Boyd, M. R.; Hamel, E.; Pettit, R. K.; Chapuis, J. C. *J. Med. Chem.* **1999**, *42*, 1459−1465. (d) Shirai, R.; Takayama, H.; Nishikawa, A.; Koiso, Y.; Hashimoto, Y. *Bioorg. Med. Chem. Lett.* **1998**, *8*, 1997−2000.

(13) Nguyen, T. L.; McGrath, C.; Hermone, A. R.; Burnett, J. C.; Zaharevitz, D. W.; Day, B. W.; Wipf, P.; Hamel, E.; Gussio, R. *J. Med. Chem.* **2005**, *48*, 6107−6116.

(14) (a) Marsault, E.; Peterson, M. L. *J. Med. Chem.* **2011**, *54*, 1961−2004. (b) Driggers, E. M.; Hale, S. P.; Lee, J.; Terrett, N. K. *Nat. Rev. Drug Discovery* **2008**, *7*, 608−624.

(15) Wang, X.; Ju, T.; Li, X.; Cao, X. *Synlett* **2010**, 2947−2949.

(16) Lomas, J. S. *Magn. Reson. Chem.* **2013**, *51*, 32−41.

(17) (a) Maya, A. B.; Pérez-Melero, C.; Mateo, C.; Alonso, D.; Fernández, J. L.; Gajate, C.; Mollinedo, F.; Peláez, R.; Caballero, E.; Medarde, M. *J. Med. Chem.* **2005**, *48*, 556−568. (b) Álvarez, R.; Puebla, P.; Díaz, J. F.; Bento, A. C.; Garcia-Navas, R.; de la Iglesia-Vicente, J.; Mollinedo, F.; Andreu, J. M.; Medarde, M.; Peláez, R. *J. Med. Chem.* **2013**, *56*, 2813−2827.

(18) (a) Shalaeva, M.; Caron, G.; Abramov, Y. A.; O'Connell, T. N.; Plummer, M. S.; Yalamanchi, G.; Farley, K. A.; Goetz, G. H.; Philippe, L.; Shapiro, M. J. *J. Med. Chem.* **2013**, *56*, 4870−4879. (b) Kuhn, B.; Mohr, P.; Stahl, M. *J. Med. Chem.* **2010**, *53*, 2601−2611.
(19) Conformational searches were performed with Macromodel v. 5.1, and clustering of the conformations was performed with XCluster on Silicon Graphics workstations.
(20) Marenich, A. V.; Olson, R. M.; Kelly, C. P.; Cramer, C. J.; Truhlar, G. H. *J. Chem. Theory Comput.* **2007**, *3*, 2011−2033.
(21) (a) Shan, Y.; Zhang, J.; Liu, Z.; Wang, M.; Dong, Y. *Curr. Med. Chem.* **2011**, *18*, 523−538. (b) Bhattacharyya, B.; Panda, D.; Gupta, S.; Banerjee, M. *Med. Res. Rev.* **2008**, *28*, 155−183.
(22) Ravelli, R. B.; Gigant, B.; Curmi, P. A.; Jourdain, I.; Lachkar, S.; Sobel, A.; Knossow, M. *Nature* **2004**, *428*, 198−202.
(23) For a complete correspondence: *ent*-I = XIV, *ent*-II = XIII, *ent*-III = XVI, *ent*-IV = XV, *ent*-V = X, *ent*-VI = IX, *ent*-VII = XII, *ent*-VIII = XI, *ent*-IX = VI, *ent*-X = V, *ent*-XI = VIII, *ent*-XII = VII, *ent*-XIII = II, *ent*-XIV = I, *ent*-XV = IV, and *ent*-XVI = III.
(24) Pettit, G. R.; Toki, B. E.; Herald, D. L.; Boyd, M. R.; Hamel, E.; Pettit, R. K.; Chapuis, J. C. *J. Med. Chem.* **1999**, *42*, 1459−1465.
(25) (a) OpenEye Scientific Software, Inc., Santa Fe, NM, www.eyesopen.com, 2012. (b) Spartan'08; Wavefunction, Inc., Irvine, CA.
(26) (a) Rappl, C.; Barbier, P.; Bourgarel-Rey, V.; Grégoire, C.; Gilli, R.; Carre, M.; Combes, S.; Finet, S. P.; Peyrot, V. *Biochemistry* **2006**, *45*, 9210−9218. (b) Nguyen, T. L.; McGrath, C.; Hermone, A. R.; Burnett, J. C.; Zaharevitz, D. W.; Day, B. W.; Wipf, P.; Hamel, E.; Gussio, R. *J. Med. Chem.* **2005**, *48*, 6107−6116.